



UNIVERSIDADE FEDERAL DO CEARÁ  
CENTRO DE TECNOLOGIA  
DEPARTAMENTO DE ENGENHARIA QUÍMICA  
CURSO DE GRADUAÇÃO EM ENGENHARIA QUÍMICA

CESAR AUGUSTO DE ARAUJO FILHO

**CATALYTIC SYNTHESIS OF PEROXYFATTY ACIDS**

Fortaleza

2010

CESAR AUGUSTO DE ARAUJO FILHO

**CATALYTIC SYNTHESIS OF PEROXYFATTY ACIDS**

Trabalho de Final de Curso submetido à  
Coordenação do Curso de Graduação em  
Engenharia Química, da Universidade Federal  
do Ceará, como requisito parcial para obtenção  
do grau de Bacharel em Engenharia Química.

Área de concentração: Catálise Heterogênea

Orientador: Dr. Fabiano André Narciso  
Fernandes

Fortaleza

2010

A658c Araujo Filho, Cesar Augusto de  
Catalytic Synthesis of Peroxyfatty Acids / Cesar Augusto de  
Araujo Filho. Fortaleza: 2010.  
47 p.; il.

Orientador: Prof. Dr. Fabiano André Narciso Fernandes  
Área de concentração: Catálise Heterogênea.  
Trabalho de Final de Curso – Universidade Federal do Ceará,  
Departamento de Engenharia Química.

1. Heterogeneous Catalysis 2. Perhydrolysis reaction  
3. Biphasic liquid system

I. Título

CDD660

CESAR AUGUSTO DE ARAUJO FILHO

CATALYTIC SYNTHESIS OF PEROXYFATTY ACIDS

Trabalho de Final de Curso submetido à Coordenação do Curso de Engenharia Química, na Universidade Federal do Ceará, como requisito parcial para obtenção do grau de Bacharel em Engenharia Química, Área de concentração: Catálise Heterogênea.

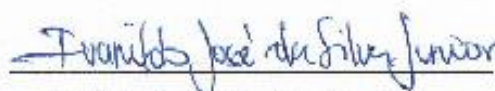
Aprovada em 17/11/2010

BANCA EXAMINADORA



Prof. Dr. Fabiano André Narciso Fernandes

Universidade Federal do Ceará



Prof. Dr. Ivanildo José da Silva Júnior

Universidade Federal do Ceará



Prof. Dr. Vitor Moreira da Rocha Ponte

Universidade Federal do Ceará



*À meus primeiros e eternos  
professores por todas as lições de amor  
e humanidade que me ensinam até hoje: Meus Pais*

## **AGRADECIMENTOS**

Em primeiro lugar, gostaria de agradecer aos meus pais César e Nazinha por todo o apoio e amor incondicional que recebi desses que são os grandes responsáveis por tudo que já conquistei. Aos meus irmãos Caio e Thiago por serem meus companheiros de todas as horas e cujas lembranças de nossas brincadeiras e bons momentos me ajudaram a superar a distância. Sem o apoio unânime de minha família este trabalho não existiria.

À CAPES e a Åbo Akademi pelo apoio financeiro durante minha estadia na Finlândia. Experiência essa de valor incomensurável para mim e cujas conseqüências trouxeram-me um amadurecimento sem precedentes.

À equipe do Laboratório de Química Industrial e Engenharia de Reações da Universidade Åbo Akademi por todo o apoio que me deram tanto em forma de orientações e suporte técnico quanto pela agradável companhia dos inúmeros encontros fora do ambiente acadêmico.

Ao meu orientador Professor Dr. Fabiano André Narciso Fernandes pela disponibilidade e perspicácia com que me colaborou para a realização deste trabalho.

Ao Professor Dr. João José Hiluy Filho pelo auxílio imprescindível nos momentos de orientação profissional e acadêmico que me fizeram crer que poderia alcançar o sonho de uma experiência internacional.

À todos os professores que tive ao longo de minha vida acadêmica e que contribuíram para minha formação.

Aos meus queridos amigos e colegas de curso com os quais tive o prazer de conviver nesses últimos anos. Agradecimentos especiais aos meus amigos Anderson Pinheiro, Jader Fernandes, Marcelo de Lima, Rodrigo Paschoal e Ronan Sousa.

Aos amigos que fiz durante o período que estive em intercâmbio cuja amizade estimo para além da distância e do tempo, são eles Ekaterina Korotkova, Elena Privalova, Jerônimo Siro, Maija Kinnunen e Nina Björkman.

*“This is not the end.  
This is not even the beginning of the end.  
But it is, perhaps, the end of the beginning.”*

Wiston Churchill

## Abstract

The perhydrolysis of valeric acid was studied in a batch reactor at 40-60°C, using Amberlite IR-120 as the heterogeneous catalyst. The reversible reaction can be illustrated as:

Two liquid phases exist in the system, one of them is polar and constituted mainly of hydrogen peroxide and water and the other one is a non-polar phase and consists mainly of valeric acid.

A study of the influence of the stirring speed and the internal mass transfer effect was done. The equilibrium constant  $K^C$  was determined for different temperatures and the enthalpy of reaction estimated by the Arrhenius equation. A kinetic model was developed taking into account the biphasic nature of the system. The mass transfer coefficients were estimated using correlations found in the literature. The energy of activation and the heterogeneous rate constant were estimated by our model.

An experimental method based in catalyst washes was used to find the concentration of components inside the catalyst particles. Although the kinetic modeling does not include this parameter yet, it will be introduced in this work due to its promising results.

**Keywords:** Heterogeneous catalysis. Perhydrolysis reaction. Biphasic liquid system.



## List of Figures

Figure 1 – Experimental apparatus.....	17
Figure 2 – Overview of equilibrium experiments.....	22
Figure 3 – Overview of kinetic experiments I.....	23
Figure 4 – Overview of kinetic experiments II .....	23
Figure 5 - Schematic picture of reaction and mass transfer phenomena .....	25
Figure 6 – External mass transfer results.....	26
Figure 7 – Internal mass transfer results .....	27
Figure 8 – Catalyst washing decay.....	28
Figure 9 – Time influence in the intra-particle concentration.....	29
Figure 10 – Intra-particle concentrations versus Bulk concentration.....	30
Figure 11 – Distribution coefficient.....	32
Figure 12 – Blank experiment.....	33
Figure 13 – Homogeneous reaction mechanism.....	34
Figure 14 – Equilibrium constant versus valeric acid molar fraction.....	37
Figure 15 – Enthalpy of reaction.....	38
Figure 16 – Diffusion coefficient of different compounds in the organic phase at different temperatures.....	45
Figure 17 – Diffusion coefficient of different compounds in the aqueous phase at different temperatures.....	45
Figure 18 – Diffusion coefficient of different compounds in the liquid-liquid system at different temperatures.....	46
Figure 19 – Mass transfer coefficients in the organic phase.....	47
Figure 20 – Mass transfer coefficients in the aqueous phase at vs $d_{32}$ .....	48
Figure 21 – Model results for the perhydrolysis of valeric acid at 60°C.....	50
Figure 22 – Model results for the perhydrolysis of valeric acid at different temperatures and catalyst loadings.....	51

## List of Tables

Table 1 – General experimental conditions .....	18
Table 2 – Catalyst properties given by the fabricants.....	20
Table 3 – Distribution coefficient.....	32
Table 4 – Kinetic parameters estimated.....	49
Table 5 – Thermodynamic parameters calculated.....	50

## List of Equations

Equation 1 – Distribution constant.....	31
Equation 2 – Gibbs free energy versus distribution constant.....	31
Equation 3 – Law of Van'T Hoff for the distribution constant.....	31
Equation 4 – Total rate of reaction.....	34
Equation 5 – Quasi-equilibrium hypothesis.....	34
Equation 6 – Discrimination of $[RC^+(OH)_2]$ .....	34
Equation 7 – Definition of the equilibrium constant for the protolysis of valeric acid.....	34
Equation 8 – Concentration of hydroxonium anions.....	34
Equation 9 – Homogeneous rate of reaction, incomplete.....	35
Equation 10 – Homogeneous rate of reaction.....	35
Equation 11 – Heterogeneous rate of reaction.....	35
Equation 12 – Total rate of reaction.....	36
Equation 13 – Reaction quotient definition.....	36
Equation 14 – Differential Law of Van't Hoff for the equilibrium constant.....	37
Equation 15 – Integrated Law of Van't Hoff for the equilibrium constant.....	38
Equation 16 – General mass balance.....	39
Equation 17 – General mass balance for the aqueous phase.....	39
Equation 18 – General equation for the Double Film Model.....	39
Equation 19 – Interfacial area.....	40
Equation 20 – Development of the aqueous mass balance.....	40
Equation 21 – Application of the distribution coefficient in the mass balance.....	40
Equation 22 – Final general mass balance for the aqueous phase.....	40
Equation 23 – Mass balance for each compound in the aqueous phase.....	40
Equation 24 - Mass balance for each compound in the aqueous phase.....	41
Equation 25 – General mass balance in the organic phase.....	41
Equation 26 – General mass balance in the organic phase.....	41

Equation 27 - Mass balance for each compound in the organic phase.....	41
Equation 28 – Sauter number.....	42
Equation 29 – Sauter number correlation.....	42
Equation 30 – Webber number.....	42
Equation 31 - Delichatsios and Probstein function.....	42
Equation 32 – Good and Girifalco’s model for the surface tension.....	43
Equation 33 – Surface tension correlation.....	43
Equation 34 - Surface tension correlation.....	43
Equation 35- Interaction parameter.....	43
Equation 36 - Perkins-Geankoplis model for the diffusion coefficient.....	44
Equation 37 – Viscosity model.....	44
Equation 38 – Viscosity correlation for the organic phase.....	44
Equation 39 – Viscosity correlation for the aqueous phase.....	44
Equation 40 – Diffusion coefficient in the aqueous phase.....	44
Equation 41 – Diffusion coefficient in organic phase.....	44
Equation 42 – Mass transfer coefficient for the organic phase.....	46
Equation 43 – Power dissipated by the stirrer.....	46
Equation 44 – Diameter $d^*$ .....	47
Equation 45 – Mass transfer coefficient for the aqueous phase.....	48
Equation 46 – Objective function .....	48
Equation 47 – General equation for a batch reactor.....	49
Equation 48 – Modified Arrhenius equation.....	49
Equation 49 – $k_{ave}$ calculation.....	49

## Contents

<b>Abstract</b> .....	<b>8</b>
<b>List of Figures</b> .....	<b>9</b>
<b>List of Tables</b> .....	<b>10</b>
<b>List of Equations</b> .....	<b>11</b>
<b>Contents</b> .....	<b>13</b>
<b>1. Introduction</b> .....	<b>15</b>
<b>2. Objectives</b> .....	<b>16</b>
<b>3. Experimental Part</b> .....	<b>17</b>
3.1 Reaction system.....	17
3.2 Catalyst washing .....	18
2.3 Analytical Method.....	19
3.4 Catalyst properties.....	19
3.4.1 Pretreatment .....	20
<b>4 Results and discussion</b> .....	<b>21</b>
4.1. Description of the system .....	21
4.1.1 Preliminary results.....	21
4.1.2 Reaction and mass transfer considerations .....	22
4.2 The influence of the rotating speed in the reaction velocity .....	25
4.3 Internal mass transfer.....	27
4.4 Concentration inside the particle .....	28
4.5 Determination of the distribution constant .....	31
4.6 Kinetics.....	33
4.7 Equilibrium analysis .....	36
4.7.1 Influence of the molar fraction in the equilibrium constant .....	36
4.7.2 Enthalpy of reaction .....	37
4.8 Mathematical model.....	39



<b>5</b>	<b>Conclusions .....</b>	<b>53</b>
<b>6</b>	<b>Acknowledgements.....</b>	<b>54</b>
<b>7</b>	<b>Notation.....</b>	<b>55</b>
<b>8</b>	<b>References .....</b>	<b>58</b>

# 1. Introduction

The peroxycarboxylic acids are commonly used as antimicrobial agents in the food manufacture, bleaching agents in textile and paper industry and in fine chemical industry (epoxidation, Bayer-Villiger reaction), all of these applications are based in the oxidative potential of these compounds, Pruss et al. (2001), Ölmez et al. (2009), Kitis (2004), Polanca et al. (2008) and Goud et al. (2007) . The low toxicity, high stability and the liquid form are features that mitigate problems like safety and waste treatment in industrial oxidation processes.

The organic chain associated with the  $-\text{COOOH}$  group makes the peroxycarboxylic acids more suitable to act in an organic media than others inorganic oxidants. According to Leveneur et al. (2009), peroxyacetic acid (PAA) is more potent antimicrobial agent than hydrogen peroxide, being rapidly active at low concentrations against a wide spectrum of micro-organisms. Moreover, PAA is a better bleaching agent compared to hydrogen peroxide, Pan et al (2000).

It is remarkable that mainly peroxyacetic and peroxypropionic acids (PPA) are used in the industrial applications of peroxycarboxylic acids and there is not much information about the perhydrolysis of fatty acids in the literature. Peroxyfatty acids are already used as bleaching agents in washing powders, Nardello-Rataj et al. (2003). In fact, they are very effective for removal of persistent yellowish stains. The solubility of its compounds in an organic solvent can be increased by the augment of the carbon chain. Therefore, one supposes that epoxidation reactions carried out with short chain peroxycarboxylic acids could be improved by using peroxyfatty acids instead, Campanella et al. (2006).



## 2. Objectives

The primary aim of this work is to verify if the perhydrolysis of fatty acids is in fact possible, since no data of such reaction is available in the literature. Once proved, it is interesting to study how the reaction rate is influenced by some key parameters such as stirring speed, particle size diameter, catalyst loading, reactants concentration and temperature. An estimation of the enthalpy of reaction can be made by an equilibrium study at different temperatures using the Van't Hoff relation. Finally, the formulation of a kinetic model comprising the liquid-liquid mass transfer effect is the most challenging step of the present work.





## 3. Experimental Part

### 3.1 Reaction system

The experiments were carried out in a 250 milliliters jacketed batch reactor and a pitched blade impeller provided a vigorous mixing of the reaction mixture (Figure 1). A carrier gas, Argonium (AGA, 99.996%), was inserted through one of the necks of the reactor in order to remove the gas compounds produced by an occasional decomposition of hydrogen peroxide (HP) or peroxyvaleric acid (VA). This gas steam must leave the system passing through a condenser at 0°C where the volatile compounds are recovered.

The reactor was washed with a solution of hydrochloric acid 10% wt. followed by another washing with a solution of 5% wt. of a phosphate-free detergent, as well as many washes with deionized water. The samples were taken with plastic syringes. All the parts in contact with the reaction mixture were carefully checked to not be contaminated with any metal, which would start the decomposition of hydrogen peroxide and the peroxyvaleric acid (PVA).

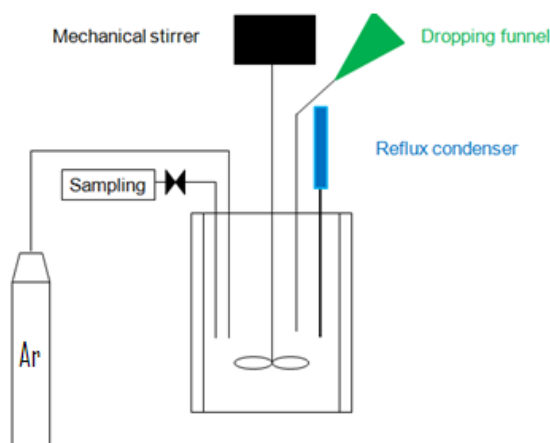


**Figure 1** - Experimental apparatus

The experiments were initiated by stirring valeric acid (Acros,  $\geq 99\%$ ) and the catalyst inside the reactor, which is been heated by the outside jacket. Meanwhile, the hydrogen peroxide (Merck,  $\geq 30\%$ ) is been preheated. When all the components achieve the



desired temperature, hydrogen peroxide is added to the reactor through a dropping funnel. This is when the time “zero” is set.

The experimental matrix is showed in Table 1.

**Table 1** - General experimental conditions

Reaction temperature [°C]	40 – 60
Catalyst loading [g.L <sup>-1</sup> ]	0 – 116
Rotating speed [rpm]	207 – 800
Initial weight percent of VA[%]	21 – 74
Initial weight percent of HP solution[%]	7 – 16
Initial weight percent of Water [%]	18 – 72

Once the reactants are mixed, an organic and an aqueous phase are formed. The aqueous phase is highly concentrated in water and hydrogen peroxide whilst the organic phase is formed basically by valeric acid. However, one can find small concentrations of hydrogen peroxide in the organic phase as well as traces of valeric acid in the aqueous phase.

The initial concentration of hydrogen peroxide and water in the aqueous phase is 2.85 – 10.85 and 37.1 – 49.2 mol.L<sup>-1</sup> respectively. In the organic phase, the initial concentration of valeric acid is 7.7 – 9.1 mol.L<sup>-1</sup>. Deionized water was used in some experiments in order to dilute the reactants.

### 3.2 *Catalyst washing*

After the reaction, the catalyst was continuously filtrated for 45 minutes. At this point, one considers that all the extra-particle liquid has been withdrawn and the intra-particle liquid remains untouched.



Thus, 100 milliliters of deionized water was poured in the filter with the catalyst and the liquid extracted was analyzed. The washing procedure was done six times for each experiment.

### **2.3 Analytical Method**

The concentrations of valeric acid and peroxyvaleric acid were determined [14] by titration with a standard solution of sodium hydroxide (0.2 N), using the Greespan and Mackellar (1948) method in an automatic titrator (Metrohm 751 GPD Titrino). A standard solution of ammonium cerium sulfate (0.1 N) was used to determine the concentration of hydrogen peroxide in the samples. Each analyze has been done twice and an average of the values is used as the final result. It is important to remark that both analyses did not differ too much from each other.

### **3.4 Catalyst properties**

The catalysts used have a styrene-divinyl benzene (gel) matrix with sulfonic groups as active sites. Leveneur et al. (2009) used it for the perhydrolysis of propionic and acetic acids and a satisfactory activity was demonstrated.

The catalysts Dowex 50Wx8-400 and Dowex 50Wx8-50 were only used for the internal mass transfer experiments. For all the others experiments Amberlite-120 was used instead.

Some properties of the catalysts are listed in Table 2.



**Table 2** – Catalyst properties given by the fabricants

	<b>Supplier</b>	<b>Polymer type</b>	<b>Moisture Content %mass</b>	<b>Capacity by dry weight meq/g</b>	<b>Cross linking %</b>	<b>Native particle size mm</b>
<b>Amberlite IR-120</b>	Aldrich	Gel	45	4.4	8	0.3-1.2
<b>Dowex 50Wx8-400</b>	Sigma-Aldrich	Gel	54	4.8	8	0.04-0.08
<b>Dowex 50Wx8-50</b>	Sigma-Aldrich	Gel	52	4.8	8	0.3-0.84

### 3.4.1 Pretreatment

A pretreatment was done in order to remove traces of impurities and release the water from the catalyst. Therefore, the catalyst was left under stirring for 2 hours in a mixture of 50% wt. water and hydrogen peroxide solution. Afterwards, it was washed with 1 liter of deionized water, filtrated and left in the oven at 99°C for 48 hours.



## 4 Results and discussion

### 4.1. *Description of the system*

Conductivity experiments were performed to investigate the nature of the dispersed and continuous phase according to the ratio VA / Water. Measurements made with valeric acid and tap water showed that under a 45% wt. of VA the continuous phase is the aqueous and over that point the continuous phase is the organic one.

#### 4.1.1 Preliminary results

Before starting the experiments one pertinent question was presented: what is the proper initial amounts of reactants that one should use to reach a reasonable production of peroxyvaleric acid? In other words, what is the better relation HP/VA that leads to a higher conversion of reactants? In this sense, equilibrium experiments carried out at 40°C and different initial ratios of HP/VA were done. The results are shown in Figure 2:

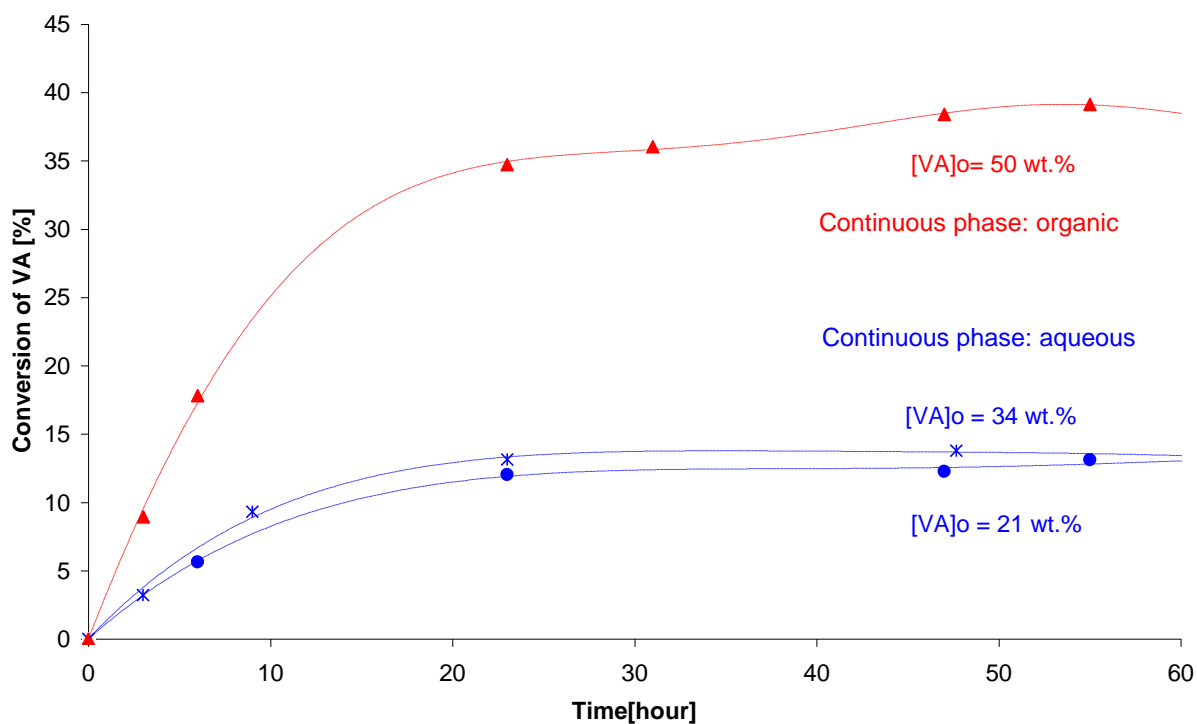


**Figure 2** - Experiments carried out at 40°C, 45 g/L of catalyst loading and 370 rpm

It is demonstrated in figure 2 that the conversion of valeric acid is considerable higher if one works with at 50% wt. instead of 34% or 21%. As a matter of fact, experiments using more than 50% wt. of VA did not achieve such high conversion, therefore, this ratio was assumed to be the optimum one.

#### 4.1.2 Reaction and mass transfer considerations

A typical graph of kinetic experiment is presented in Figure 3 and Figure 4. These graphs show separately the result of an experiment carried out at 60°C, 370 rpm and 43 g/L of catalyst loading.

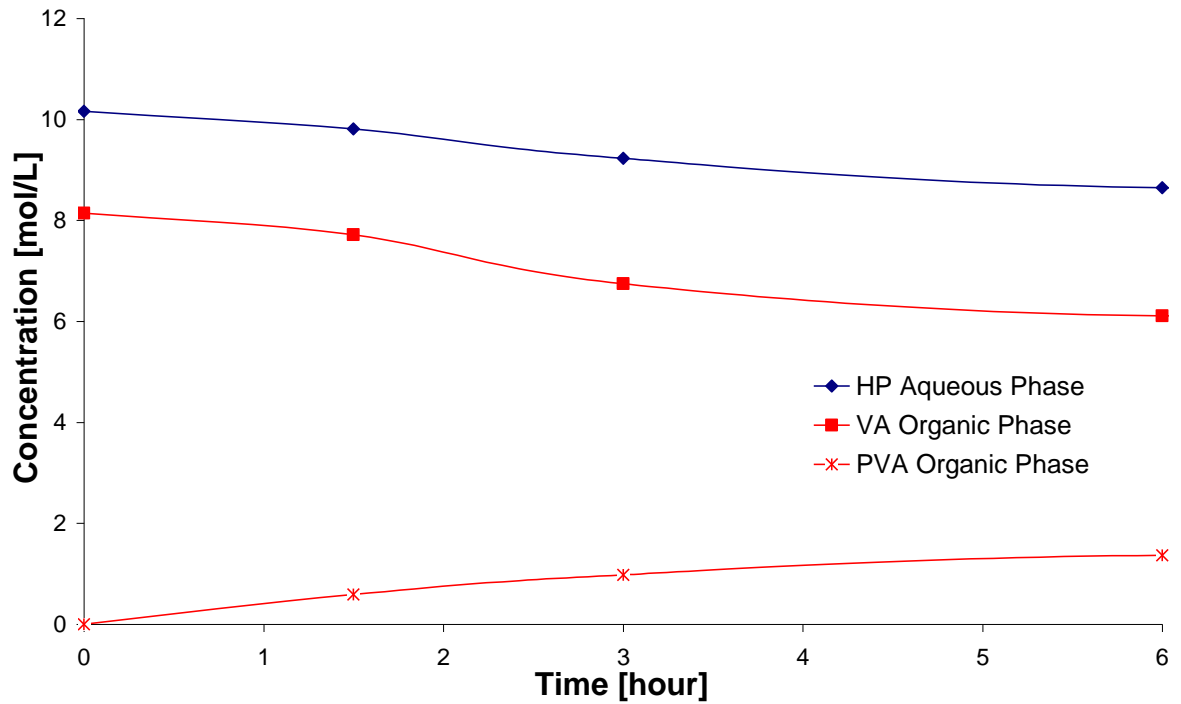


Figure 3 – Species which undergo into some significant concentration variation along the reaction time.

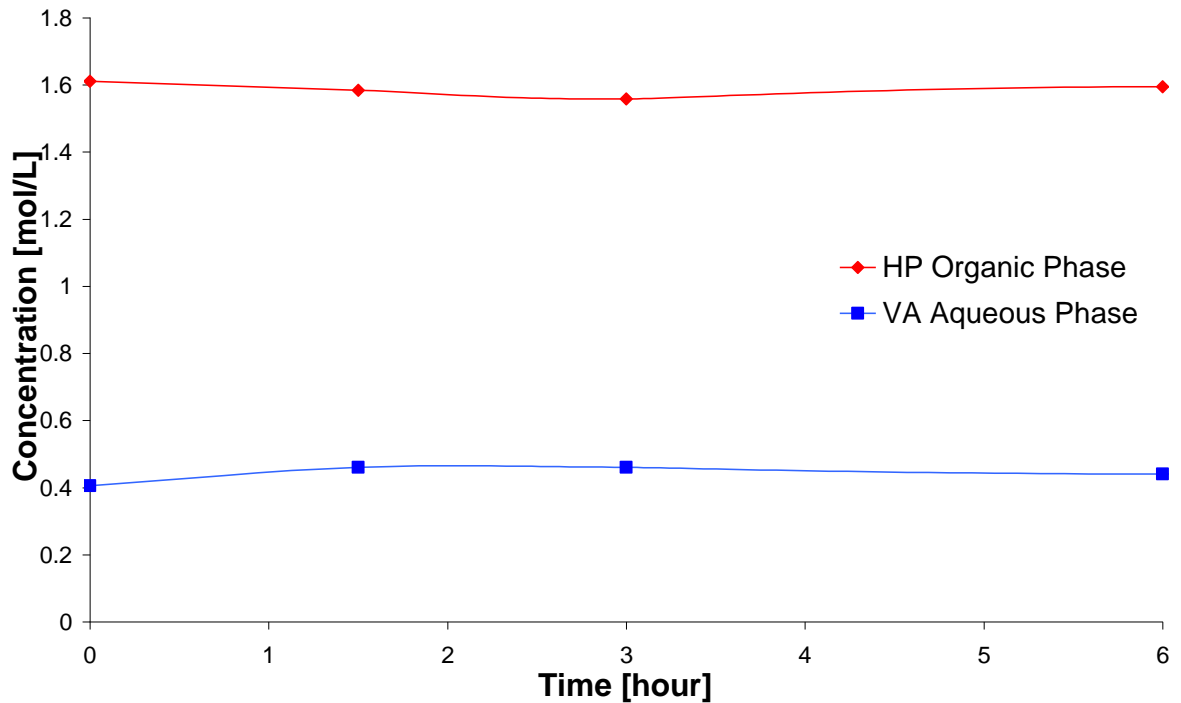


Figure 4 - Species which do not undergo into some significant concentration variation along the reaction time.



It can be noticed in figure 3 that only hydrogen peroxide from the aqueous phase and valeric acid from the organic phase are consumed along the reaction. From figure 4, one observes that hydrogen peroxide from organic phase and valeric acid from aqueous phase remain constant. The peroxyvaleric acid was only detected in the organic phase, although Nuclear Magnetic Resonance analyses were performed in the aqueous phase but it was not successful to distinguish PVA and VA neither water and HP molecules. The behavior seen in figures 3 and 4 was observed in all the experiment.

The assumptions made about the reaction and mass transfer phenomena are listed as follows:

- The production of peroxyvaleric acid due to the dissociation of valeric occurs mainly in the organic phase.
- The production of peroxyvaleric acid is mainly catalyzed by the active sites of the catalyst.
- For the sake of simplicity, the diffusion of components towards and out of the particle was not taken into account.
- Water and hydrogen peroxide from the aqueous phase diffuse to the organic phase.
- Valeric acid from the organic phase diffuses to the aqueous phase.
- Peroxyvaleric acid did not undergo in the inter-phase mass transfer.

A schematic illustration of the system is shown in Figure 5.



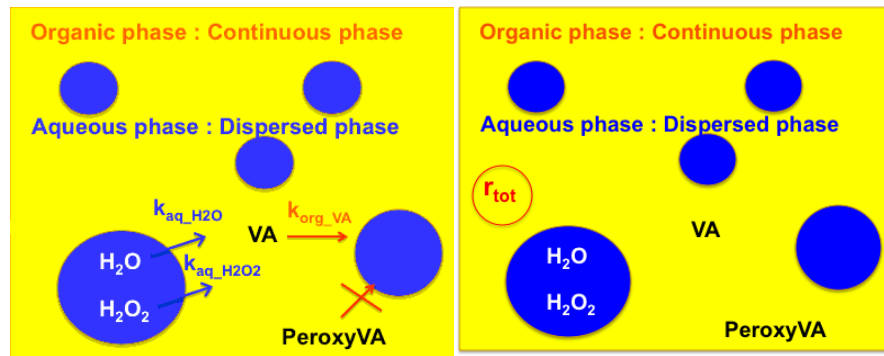


**Figure 5** - Mass transfer phenomena and reaction are illustrated here by two different pictures, even though both happen at the same time.

#### 4.2 *The influence of the rotating speed in the reaction velocity*

The influence of the stirring speed should be investigated in our system since the perhydrolysis of valeric acid occurs in a biphasic liquid media. A prove experiment was prepared in order to observe how the catalyst particles move inside the reactor. Then, it was noticed that below 207 rpm the particles could not be lifted and spread all over the reactant mixture. Furthermore, over 800 rpm the system gets too much instable and some catalyst starts to be launched to the top of the reactor.

The results obtained are shown in figure 6.

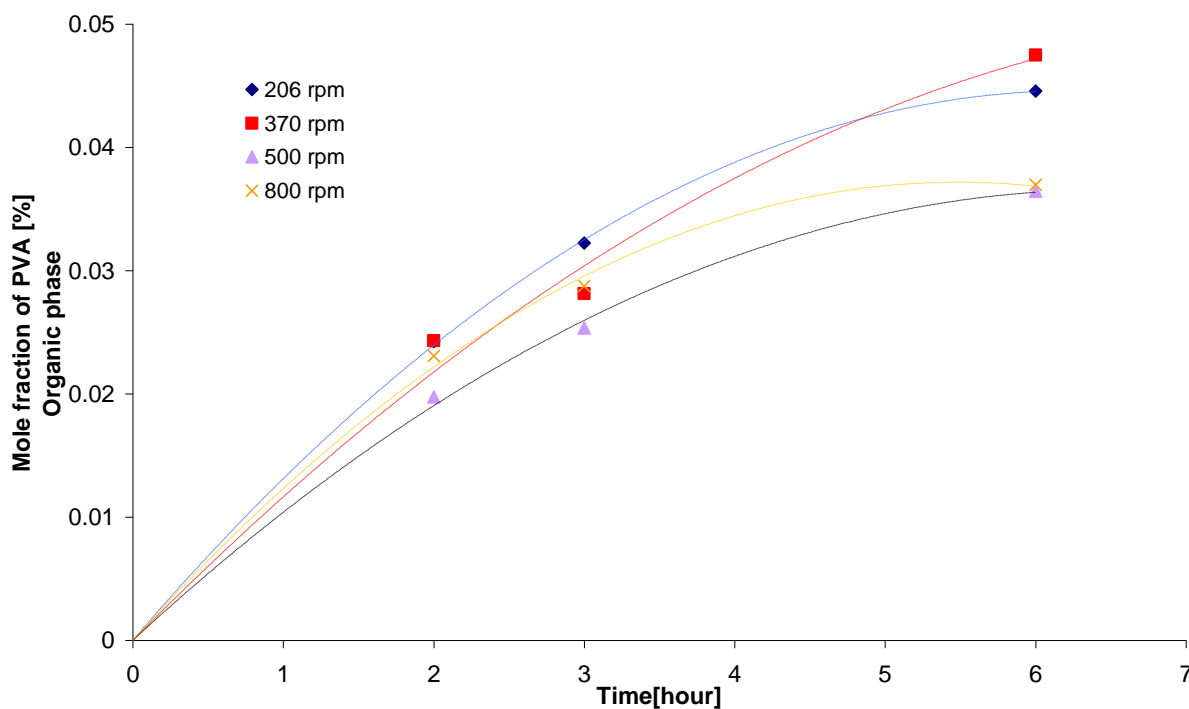


**Figure 6** - Experiments carried out at 60°C, 50% wt. VA and 43 g/L of catalyst loading.

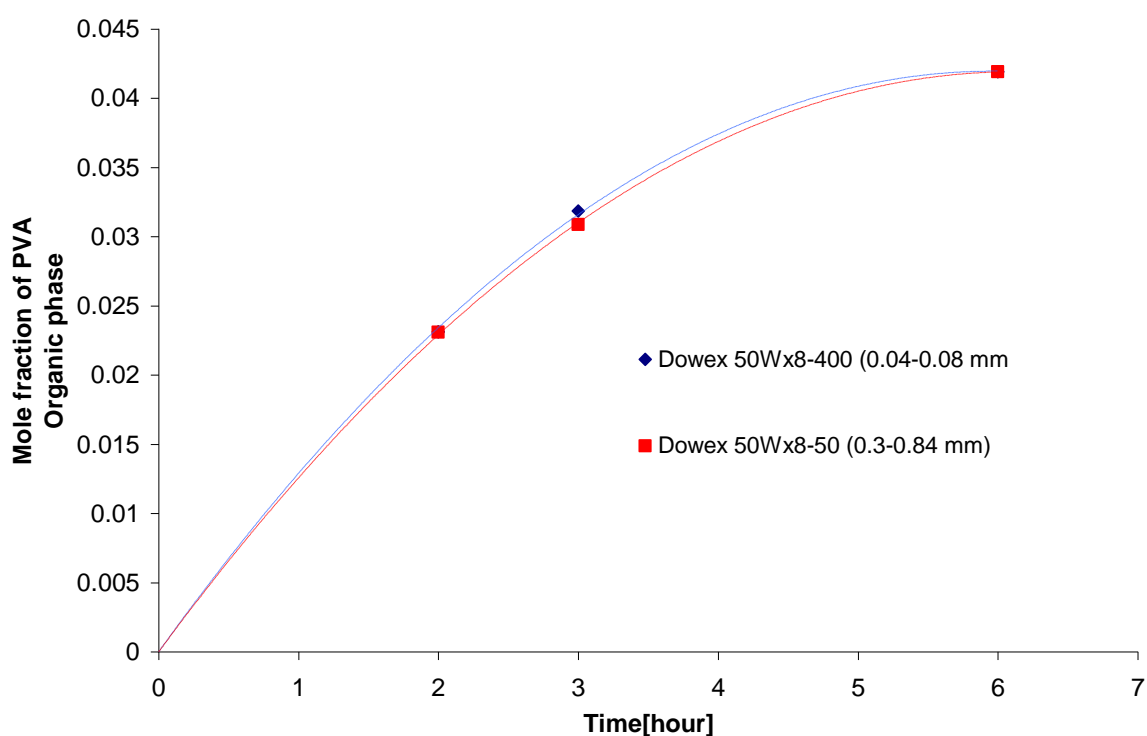
It was observed that at 500 and 800 rpm the mole fraction of PVA in the end of the reaction is clearly smaller compared to the others experiments. It is probably due to the high stirring speed which forms a vortex in the reactor pushing the catalyst against the walls. This phenomenon is not desired because the catalyst will not be uniformly distributed in the reaction mixture, causing the decrease in the conversion and kinetics of the reaction. However, the 206 and 370 rpm rotating speeds have a quite similar behavior which indicates these experiments are already in the kinetic regime. Therefore, the 370 rpm was the rotating speed used in all the other experiments.



### 4.3 Internal mass transfer

The internal mass transfer effect was studied by comparing kinetic experiments with Dowex 50Wx8-400 and Dowex 50Wx8-50. In spite of these materials are not strictly similar to Amberlite IR-120, the crosss-linking, which is the parameter governing the diffusion, is identical in all of them. Catalyst properties were listed in Table 2.

The results are shown in Figure 7.



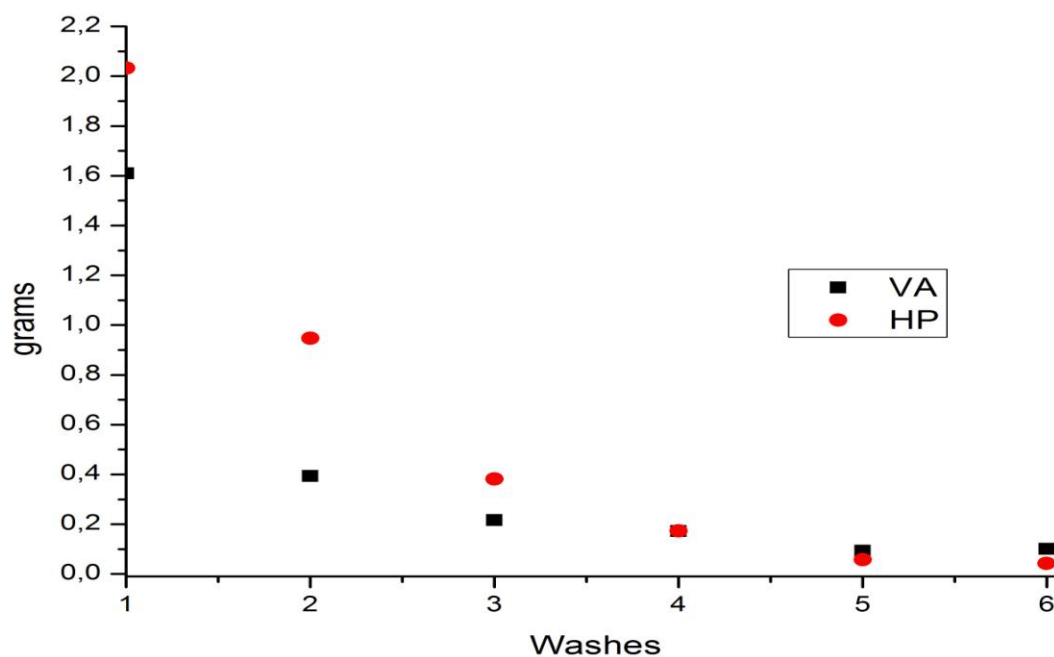
**Figure 7** - Influence of the mass transfer on the mole fraction of PVA at 60°C and 370 rpm of stirring speed.

Figure 7 shows that the effect of the internal mass transfer can be neglected in our reaction system. Leveneur et al. (2009) used the same heterogeneous catalysts in the perhydrolysis of acetic and propionic acids and the internal mass transfer limitation was found to be non-negligible in that case. This might be due to the faster kinetics of the small carbon chain carboxylic acids Musante et al. (2000).



#### 4.4 Concentration inside the particle

Figure 8 illustrates the amounts of VA and HP found in each catalyst wash for a reaction performed at 60°C, 50% wt. of VA and 43 g/L of initial catalyst loading.



**Figure 8** - Grams of HP and VA extracted after a series of 6 washes.

This is a typical curve of the catalyst washing procedure. One assumes that after the sixth wash the amounts of VA and HP are negligible for the calculation.

Prove experiments were done in order to have a better understanding of how the concentration inside the particle varies with the time. The result is shown in Figure 9:

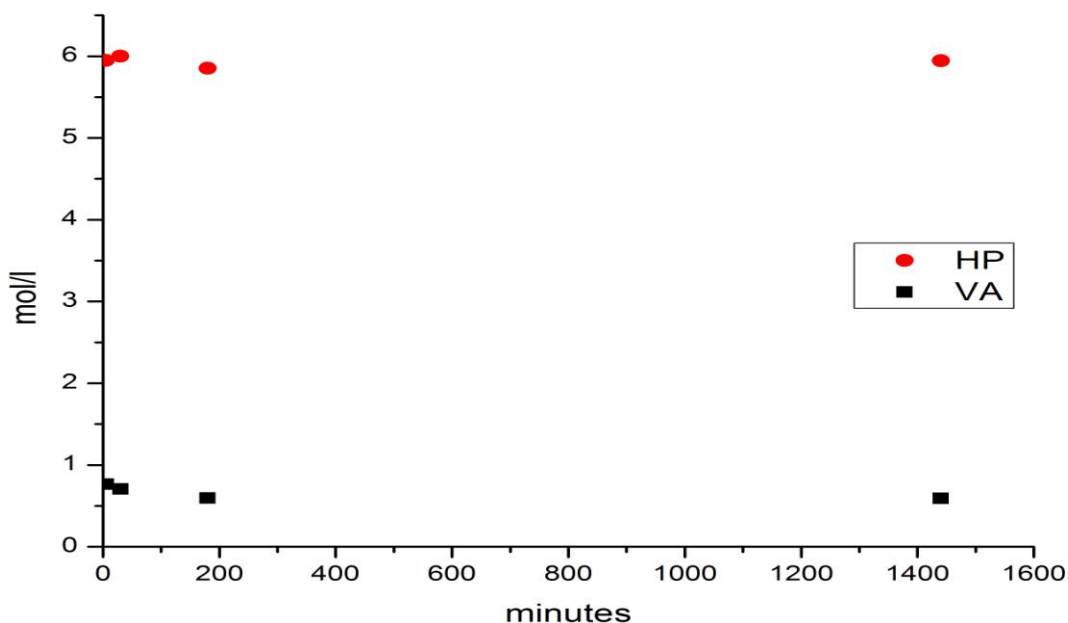


**Figure 9** - Experiments performed at 25°C with 50% wt. of VA and 45 g/L of catalyst loading.

Figure 9 shows that the time has no influence in the concentration inside the catalyst.

It was noticed that the concentration inside the catalyst is not dependent on the temperature and catalyst loading. However, the concentration in the bulk phase showed a particular influence on it.

Four experiments performed using 45-55% wt. of VA and different proportions of HP were compared and the results are shown in figure 10. These experiments were carried out under the same temperature, rotating speed and catalyst loading. The concentrations of HP are measured in the aqueous phase and the VA in the organic phase, both at the end of the reaction.

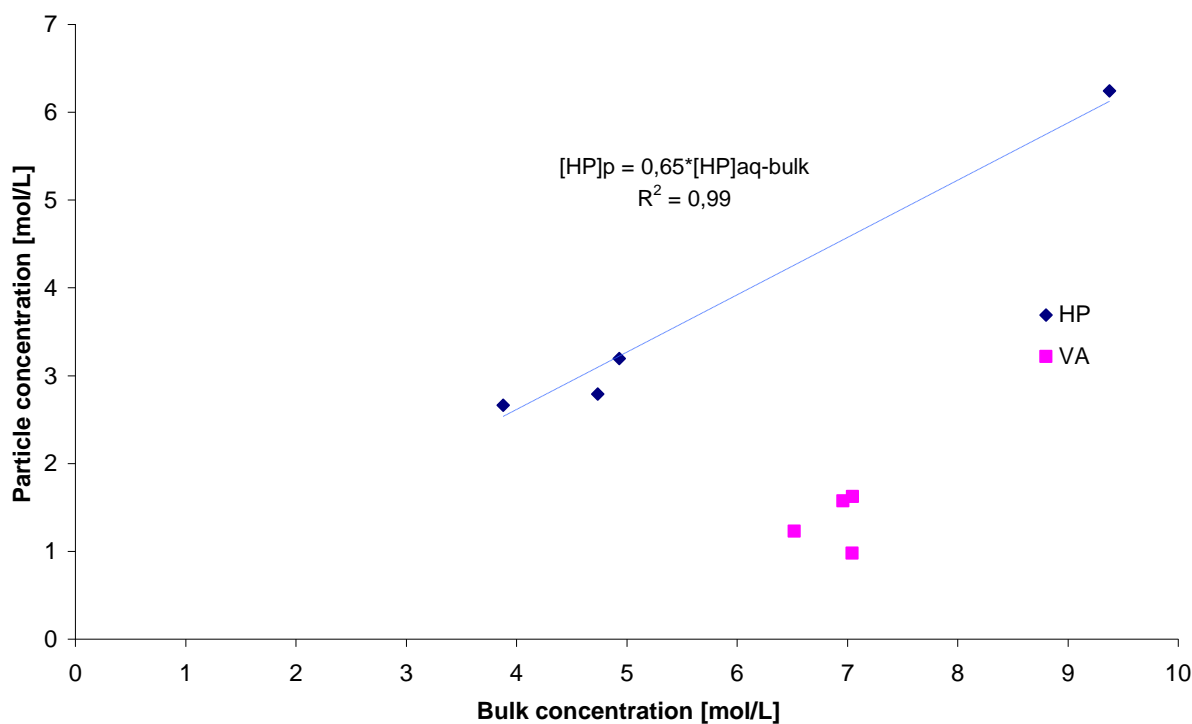


**Figure 10** - Relationship between the bulk and intra-particle concentrations.

The initial amount of valeric acid was kept under a small range of values, so did its intra-particle concentration. However, a linear relation was found in the case of hydrogen peroxide, which is in agreement with the behavior found by Musante et al. (2000) when studying the epoxidation of vegetable oils with peracetic acid using Amberlite-120.

Further investigations in this topic are needed in order to find the general relations between the bulk and intra-particle concentrations for the components in the reaction mixture and finally insert this information in the kinetic model. However, the results got so far point to a promising study.



#### 4.5 Determination of the distribution constant

The distribution constant of the species  $i$  is defined as:

$$K_i = \frac{[i]_{\text{org}}}{[i]_{\text{aq}}} \quad (1)$$

Where the concentrations are calculated at the equilibrium.

As the liquid-liquid equilibrium is a chemical thermodynamic system, the  $K_i$  is related to a Gibbs energy:

$$K_i = \exp\left(\frac{-\Delta G}{RT}\right) \quad (2)$$

The law of Van't Hoff describes the temperature dependence of  $K_i$ :

$$\ln \frac{K_i(T)}{K_i(T_{\text{ref}})} = \frac{-\Delta H_R^\circ}{R} \exp\left(\frac{1}{T} - \frac{1}{T_{\text{ref}}}\right) \quad (3)$$

Figure 11 shows the plot of  $\ln(K_i(T))$  versus  $-1/RT$ .

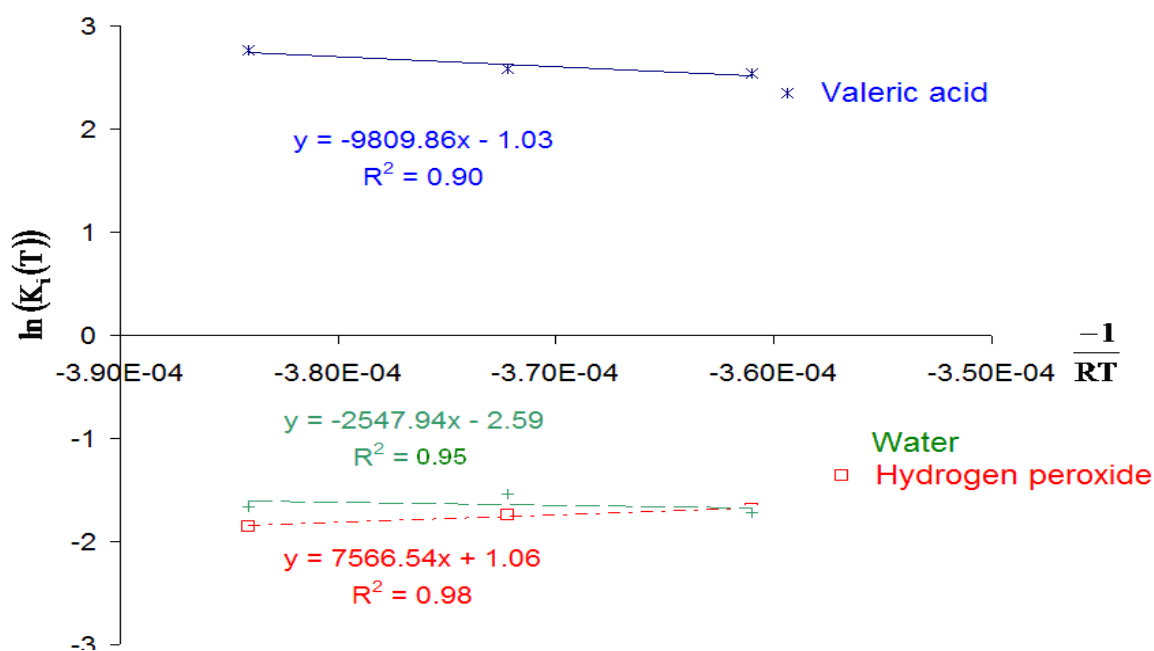


**Figure 11** - Experiments carried out at 50% of VA and 45g/L of catalyst loading.

**Table 3** - Distribution coefficient of different compounds in different temperatures with a solution of 50% of VA

$K = [i]_{org}/[i]_{aqu}$			
Temperature °C	Valeric acid	H <sub>2</sub> O <sub>2</sub>	Water
40	15.86	0.16	0.19
50	13.23	0.18	0.21
60	12.66	0.19	0.18

As the peroxyvaleric acid was not detected in the aqueous phase in any experiment  $K_{PVA}$  was not taken under consideration.





## 4.6 Kinetics

According to Leveneur et al. (2009), the perhydrolysis reaction catalyzed by cation exchange resins can be divided into two different parts: the self-catalyzed reaction due to the protolysis of the carboxylic acid and an Eley-Rideal mechanism with the adsorption of the carboxylic acid on the sulfonic group.

The range of concentration used for the kinetic experiments varied between 48-55% wt. of valeric acid. In these cases, the continuous phase was the organic and the dispersed one was the aqueous.

A blank experiment was performed in order to study how the reaction system behaves in the absence of catalyst. The result is shown in figure 12.

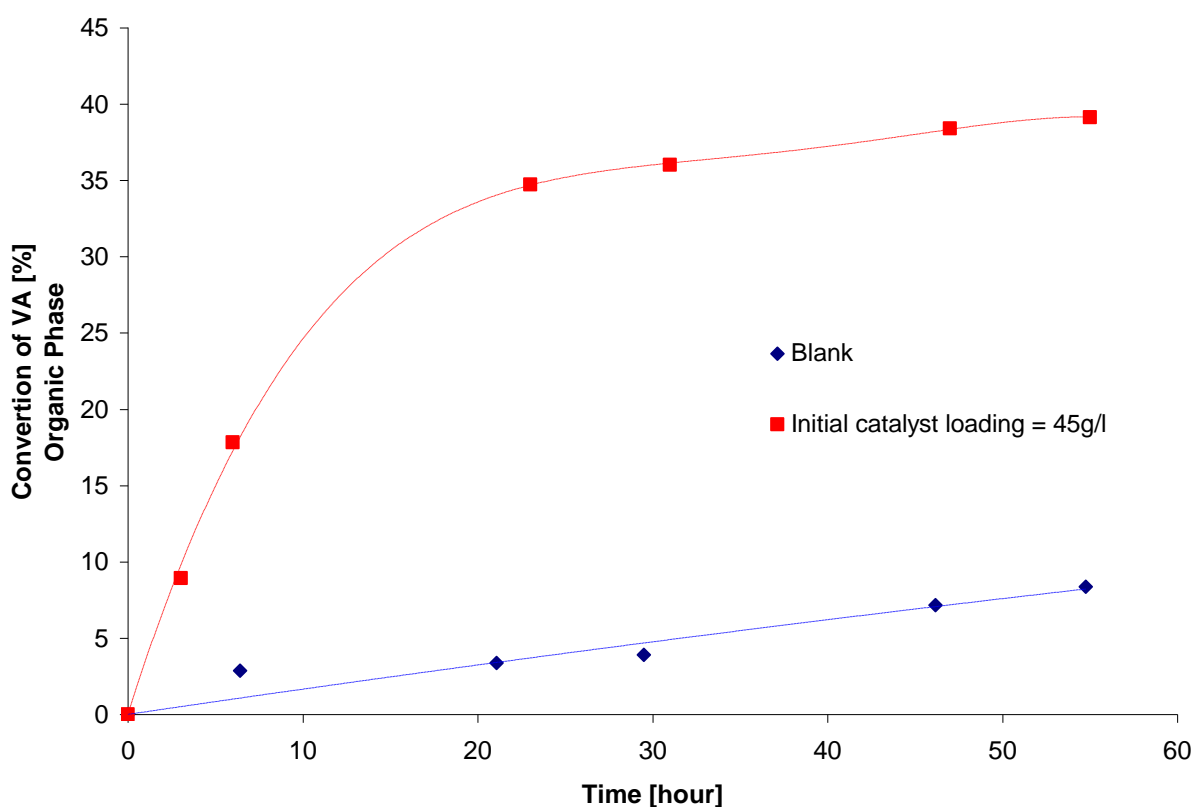


**Figure 12** - Conversion of valeric acid in the blank experiment at 45 g/L of catalyst loading. Both experiments were carried out at 50% wt. of VA and 370 rpm.



Figure 12 shows that even in the absence of catalyst the perhydrolysis of valeric acids takes place in our system. Therefore, the influence of the self-catalyzed reaction could not be neglected in our model.

The total rate of reaction can be described as:

$$r_{\text{tot}} = r_{\text{hom}} + r_{\text{het}} \quad (4)$$

The proposed mechanism for the homogeneous reaction is presented in Figure 13.

1.  $\text{RCOOH} + \text{H}_2\text{O} \rightleftharpoons \text{RCOO}^- + \text{H}_3\text{O}^+$
2.  $\text{RCOOH} + \text{H}_3\text{O}^+ \rightleftharpoons \text{RC}^+(\text{OH})_2 + \text{H}_2\text{O}$
3.  $\text{RC}^+(\text{OH})_2 + \text{H}_2\text{O}_2 \rightleftharpoons \text{RCO}_3\text{H} + \text{H}_3\text{O}^+$

**Figure 13** - Simplified mechanism for the self-catalyzed perhydrolysis reaction.

The quasi-equilibrium hypothesis is applied for the reversible proton donor reaction (reaction number 2 in Fig. 13). This assumption implies that

$$k_{+2} * [\text{RCOOH}] * [\text{H}_3\text{O}^+] \approx k_{-2} * [\text{RC}^+(\text{OH})_2] * [\text{H}_2\text{O}] \quad (5)$$

By noting the ratio  $\frac{k_{+2}}{k_{-2}}$  is equal to  $K_2^C$ , the concentration of the intermediate

$\text{RC}^+(\text{OH})_2$  is obtained from

$$[\text{RC}^+(\text{OH})_2] = \frac{K_2^C * [\text{RCOOH}] * [\text{H}_3\text{O}^+]}{[\text{H}_2\text{O}]} \quad (6)$$

The concentration-based equilibrium constant  $K_1^C$  is defined as

$$K_1^C = \frac{[\text{RCOO}^-] * [\text{H}_3\text{O}^+]}{[\text{RCOOH}] * [\text{H}_2\text{O}]} \quad (7)$$

It is reasonable to assume that  $[\text{RCOO}^-] = [\text{H}_3\text{O}^+]$  since the protolysis of valeric acid (reaction 1) is very much significant than the subsequent reactions, then Eq. (7) becomes

$$[\text{H}_3\text{O}^+] = \sqrt{K_1^C [\text{RCOOH}] [\text{H}_2\text{O}]} \quad (8)$$



The rate-determining step for the homogeneous system is the reversible reaction 3, and the rate  $r_{\text{hom}}$  can now be expressed as

$$\begin{aligned}
 r_{\text{hom}} = r_3 &= k_{+3} * [\text{RC}^+(\text{OH})_2] * [\text{H}_2\text{O}_2] - k_{-3} * [\text{RCO}_3\text{H}] * [\text{H}_3\text{O}^+] \\
 &= \frac{k_{+3} * K_2^C * \sqrt{K_1^C * [\text{RCOOH}] * [\text{H}_2\text{O}]}}{[\text{H}_2\text{O}]} * \left( [\text{RCOOH}] * [\text{H}_2\text{O}_2] - \frac{1}{K_2^C K_3^C} * [\text{RCO}_3\text{H}] * [\text{H}_2\text{O}] \right)
 \end{aligned} \tag{9}$$

Where the equilibrium constant  $K_3^C$  is equal to the ratio  $\frac{k_{+3}}{k_{-3}}$ . The products  $k_{+3} * K_2^C$  and  $K_2^C * K_3^C$  are denoted by the merged constants  $k_{\text{hom}}$  and  $K_{\text{hom}}^C$ , respectively. Then, Eq. (9) becomes

$$r_{\text{hom}} = r_3 = \frac{k_{\text{hom}} \sqrt{K_1^C * [\text{RCOOH}] * [\text{H}_2\text{O}]}}{[\text{H}_2\text{O}]} * \left( [\text{RCOOH}] * [\text{H}_2\text{O}_2] - \frac{1}{K_{\text{hom}}^C} * [\text{RCO}_3\text{H}] * [\text{H}_2\text{O}] \right) \tag{10}$$

For the heterogeneous part, it was used the same approach as Musante et al. (2000) by assuming a pseudo homogeneous model:

$$r_{\text{het}} = k_{\text{het}} * CL * \left( [\text{RCOOH}] * [\text{H}_2\text{O}_2] - \frac{1}{K_{\text{hom}}^C} * [\text{RCO}_3\text{H}] * [\text{H}_2\text{O}] \right) \tag{11}$$

Where the CL is the catalyst loading and it is expressed in grams of dry catalyst per cubic meters of organic phase.

Indeed, equations like (11) occur frequently in heterogeneous catalysis as a simple way to take the mass of catalyst into account.

The global equilibrium constant for homogeneous and heterogeneous system was assumed to be equal.

Finally, the total rate of reaction can be expressed as



$$r_{tot} = \left( \frac{k_{hom} \sqrt{K_1^C * [RCOOH] * [H_2O]}}{[H_2O]} + k_{het} * CL \right) * \left( [RCOOH] * [H_2O_2] - \frac{1}{K_{hom}^C} * [RCO_3H] * [H_2O] \right) \quad (12)$$

The value of  $K_1^C$  was calculated by using the equation from Sue et al. (2004). The apparent rate constant for the homogeneous reaction was calculated from different blank experiments carried for a long reaction time.

## 4.7 Equilibrium analysis

### 4.7.1 Influence of the molar fraction in the equilibrium constant

Perhydrolysis reactions are governed by equilibrium constant. In order to determine the thermodynamics parameters of our reaction an equilibrium study is necessary.

The equilibrium constant was determined by analysis of the reaction quotient, defined as:

$$Q = \frac{[PVA]_{org} [H_2O]_{org}}{[VA]_{org} [H_2O_2]_{org}} \quad (13)$$

Once this parameter becomes constant one assumes that the equilibrium is attained and at this point  $Q$  is equal to  $K^C$ . Bucalà et al. (2006) have demonstrated that in case of liquid-liquid system the thermodynamic equilibrium constant in the organic and aqueous phase are equal, however in our case, as no PVA was detected in the aqueous phase, it was assumed that no reaction occurs there. Figure 14 illustrates how the value of  $K^C$  varies with the initial molar fraction of VA.

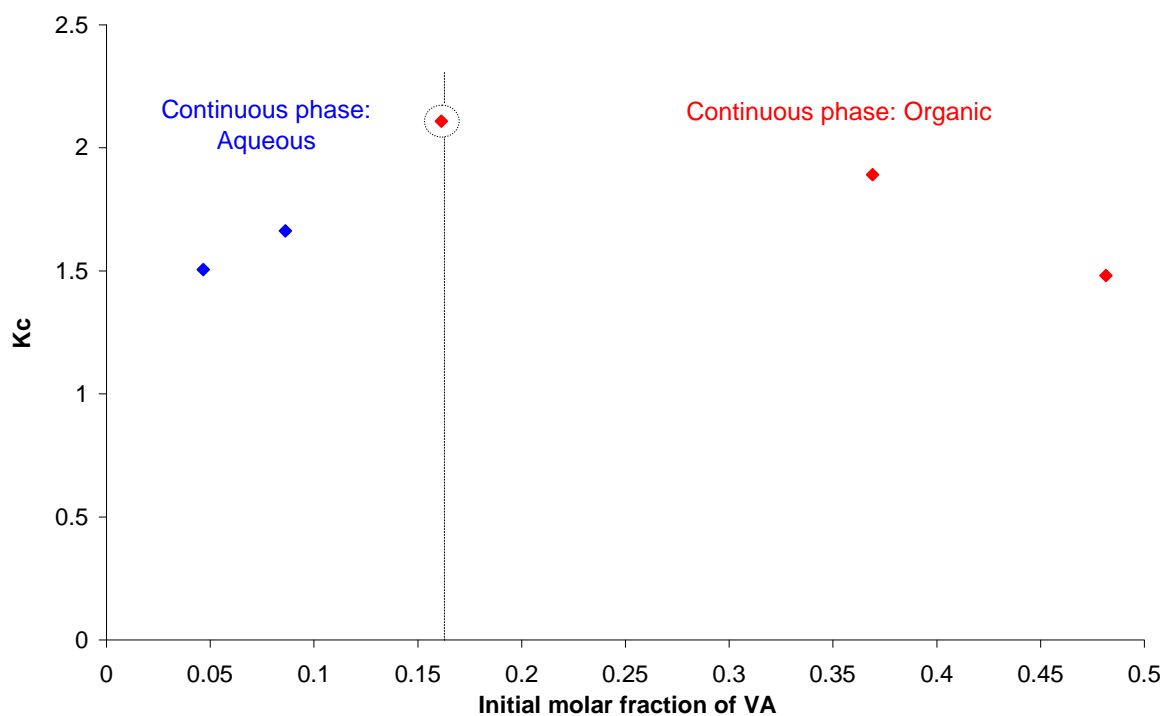


**Figure 14** - Experiments carried out at 40°C and 45 g/l of catalyst loading

The equilibrium constant reaches a maximum in the molar fraction of 0.161 of VA. This behavior can be accredited to the non-ideality of the system which inverts the dispersed and continuous phase at this point.

#### 4.7.2 Enthalpy of reaction

For the sake of simplicity, one assumes that  $K^C$  is equivalent to the true thermodynamic constant  $K^T$ . Thus,  $K^T$  can be described by the law of Van't Hoff:

$$\frac{d \ln K^T}{dT} = -\frac{\Delta H_r^o}{RT^2} \quad (14)$$



By integrating the (14) from a particular temperature  $T_{ref}$  to an arbitrary  $T$  and considering the enthalpy of reaction to be constant in the range of 40-60 °C, one finds the following relation:

$$\ln \frac{K^T}{K_{ref}^T} = \frac{-\Delta H_r^o}{R} \left( \frac{1}{T} - \frac{1}{T_{ref}} \right) \quad (15)$$

An estimation of the enthalpy of reaction was done by comparing experiments carried out with 50% wt. VA at 40, 50 and 60°C. The results are shown in figure 15.

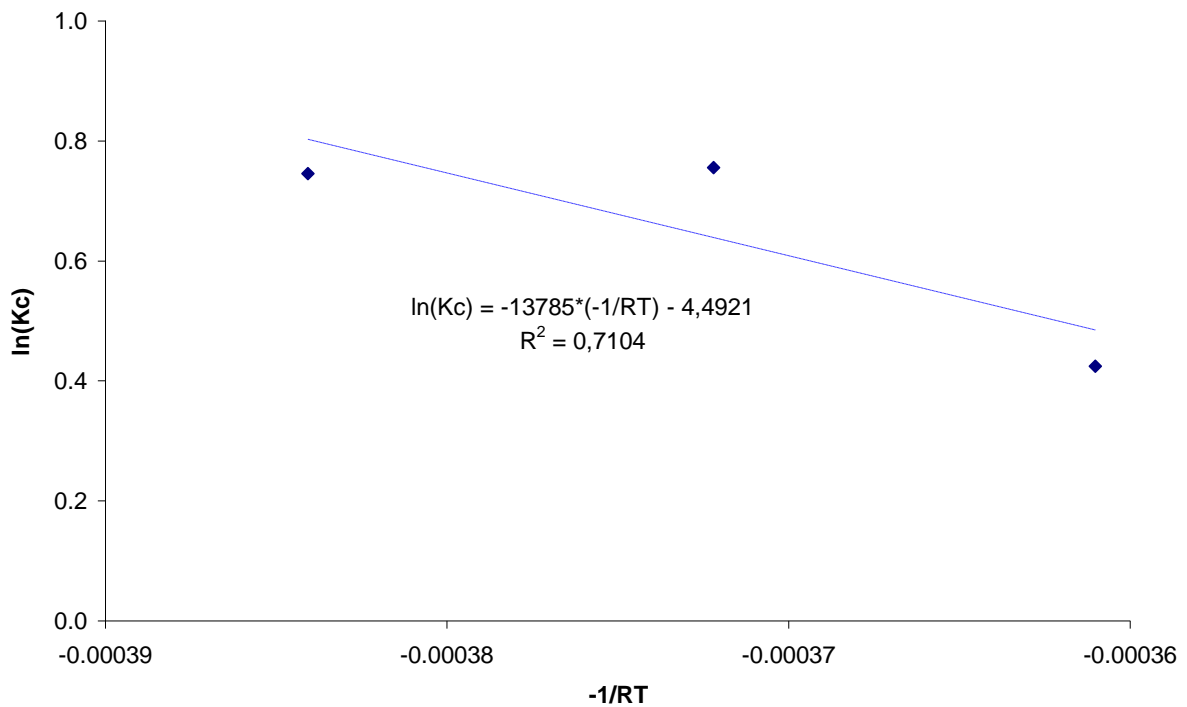


**Figure 15** - Plot  $\ln(K_{org}^C)$  versus  $-1/RT$  with  $X_{VA}$  equal to 0.16

Finally, the enthalpy of reaction was approximated to -13.8 kJ/mol.



## 4.8 *Mathematical model*

The heterogeneous and homogeneous reactions were assumed to happen in the organic phase and the catalyst was treated only as a promoter of the reaction, no diffusion towards or out of the particle was assumed to occur.

For the sake of simplicity, the water and hydrogen peroxide from the aqueous phase diffuse to the organic phase (characterized by the mass transfer coefficient  $k_{p-i}$ ); valeric acid from the organic phase diffuses to the aqueous phase (characterized by the mass transfer coefficient  $k_{c-i}$ ); since no peroxyvaleric acid was detected in the aqueous phase, its phase transfer was neglected.

### *Mass balance in the aqueous phase*

The general mass balance for any compounds (i) in the aqueous phase is:

$$N_{\text{org}}(i)A_{\text{aq/org}} = N_{\text{aq}}(i)A_{\text{aq/org}} + \frac{dn_{\text{aq}}(i)}{dt} + r_{\text{tot}} \quad (16)$$

As  $r_{\text{tot}}$  is zero in the aqueous phase, (16) becomes

$$\frac{dn_{\text{aq}}(i)}{dt} = (N_{\text{org}}(i) - N_{\text{aq}}(i))A_{\text{aq/org}} \quad (17)$$

Where the  $A_{\text{aq/org}}$  is the interfacial area between the liquid-liquid system.

The law of Fick describes the interfacial mass transfer, so:

$$\begin{aligned} N_{\text{org}}(i) &= k_{\text{org-i}}(c_{\text{org}}^*(i) - c_{\text{org}}(i)) \\ N_{\text{aq}}(i) &= k_{\text{aq-i}}(c_{\text{aq}}(i) - c_{\text{aq}}^*(i)) \end{aligned} \quad (18)$$

Where  $c^*(i)$  is the concentration in the liquid-liquid interface,  $k_x(i)$  is the mass transfer coefficient of the compound (i) in the X phase.

The interfacial area between the organic and the aqueous phase is introduced as the parameter  $a_0$ :



$$a_o = \frac{A_{aq/org}}{V_{o,tot}} \Leftrightarrow A_{aq/org} = V_{o,tot} a_o \quad (19)$$

Where  $V_{o,tot}$  is the total volume of organic and liquid phase measured in the end of the reaction. The calculation of the mass transfer coefficients will be discussed later.

By inserting the equations (18) and (19) in (17),

$$\frac{dn_{aq}(i)}{dt} = \left( k_{org-i} (c_{org}^* - c_{org}) + k_{aq-i} (c_{aq} - c_{aq}^*) \right) a_o V_{o,tot} \quad (20)$$

The concentration at the aqueous-organic interface is obtained from:

$$K_i = \frac{c_{org}^*}{c_{aq}^*} \approx \left( \frac{c_{org}}{c_{aqu}} \right)_{equilibrium} \quad (21)$$

Where  $K_i$  is the distribution coefficient of the compound (i).

Therefore, (20) becomes

$$\frac{dn_{aq}(i)}{dt} = \left( k_{org-i} (K_i c_{aq} - c_{org}) + k_{aq-i} \left( c_{aq} - \frac{c_{org}}{K_i} \right) \right) a_o V_{o,tot} \quad (22)$$

Applying equation (22) to the species present in the aqueous phase, one obtains the following system:

$$\begin{aligned} \frac{dn_{aq}(VA)}{dt} &= \left( k_{org-VA} (K_{VA} [VA]_{aq} - [VA]_{org}) \right) a_o V_{o,tot} \\ \frac{dn_{aq}(H_2O)}{dt} &= \left( -k_{aq-H_2O} \left( [H_2O]_{aq} - \frac{[H_2O]_{org}}{K_{H_2O}} \right) \right) a_o V_{o,tot} \\ \frac{dn_{aq}(H_2O_2)}{dt} &= \left( -k_{aq-H_2O_2} \left( [H_2O_2]_{aq} - \frac{[H_2O_2]_{org}}{K_{H_2O_2}} \right) \right) a_o V_{o,tot} \end{aligned} \quad (23)$$

The system (23) can be rearranged to:





$$\begin{aligned}
 \frac{d[\text{VA}]_{\text{aq}}}{dt} &= a_o \frac{V_{o,\text{tot}}}{V_{\text{aq}}} \left[ k_{\text{org-VA}} \left( K_{\text{VA}} [\text{VA}]_{\text{aq}} - [\text{VA}]_{\text{org}} \right) \right] \\
 \frac{d[\text{H}_2\text{O}]_{\text{aq}}}{dt} &= -a_o \frac{V_{o,\text{tot}}}{V_{\text{aq}}} \left( k_{\text{aq-H}_2\text{O}} \left( [\text{H}_2\text{O}]_{\text{aq}} - \frac{[\text{H}_2\text{O}]_{\text{org}}}{K_{\text{H}_2\text{O}}} \right) \right) \\
 \frac{d[\text{H}_2\text{O}_2]_{\text{aq}}}{dt} &= -a_o \frac{V_{o,\text{tot}}}{V_{\text{aq}}} \left( k_{\text{aq-H}_2\text{O}_2} \left( [\text{H}_2\text{O}_2]_{\text{aq}} - \frac{[\text{H}_2\text{O}_2]_{\text{org}}}{K_{\text{H}_2\text{O}_2}} \right) \right)
 \end{aligned} \tag{24}$$

### Mass balance in the organic phase

The mass balance of the compound (i) in the organic phase is

$$N_{\text{aq}}(\text{i})A_{\text{aq/org}} + v(\text{i})r_{\text{tot}}V_{\text{org}} = N_{\text{org}}(\text{i})A_{\text{aq/org}} + \frac{dn_{\text{org}}(\text{i})}{dt} \tag{25}$$

Rearranging (25):

$$\frac{dn_{\text{org}}(\text{i})}{dt} = v(\text{i})r_{\text{tot}}V_{\text{org}} + (N_{\text{aq}}(\text{i}) - N_{\text{org}}(\text{i}))A_{\text{aq/org}} \tag{26}$$

Applying (26) to the species present in the organic phase, one obtains the following system:

$$\begin{aligned}
 \frac{d[\text{VA}]_{\text{org}}}{dt} &= -a_o \frac{V_{o,\text{tot}}}{V_{\text{org}}} \left[ k_{\text{org-VA}} \left( K_{\text{VA}} [\text{VA}]_{\text{aq}} - [\text{VA}]_{\text{org}} \right) \right] - r_{\text{tot}} \\
 \frac{d[\text{H}_2\text{O}]_{\text{aq}}}{dt} &= a_o \frac{V_{o,\text{tot}}}{V_{\text{org}}} \left[ k_{\text{aq-H}_2\text{O}} \left( [\text{H}_2\text{O}]_{\text{aq}} - \frac{[\text{H}_2\text{O}]_{\text{org}}}{K_{\text{H}_2\text{O}}} \right) \right] + r_{\text{tot}} \\
 \frac{d[\text{H}_2\text{O}_2]_{\text{org}}}{dt} &= a_o \frac{V_{o,\text{tot}}}{V_{\text{aq}}} \left[ k_{\text{aq-H}_2\text{O}_2} \left( [\text{H}_2\text{O}_2]_{\text{aq}} - \frac{[\text{H}_2\text{O}_2]_{\text{org}}}{K_{\text{H}_2\text{O}_2}} \right) \right] - r_{\text{tot}} \\
 \frac{d[\text{PVA}]_{\text{org}}}{dt} &= r_{\text{tot}}
 \end{aligned} \tag{27}$$



*Calculation of the interfacial area between the organic and aqueous phase  $a_0$*

The following expression was used to calculate the parameter  $a_0$  (van Woezik and Westerterp, 2000; Zaldívar et al., 1996; Campanella and Baltanás, 2007):

$$a_0 = \frac{6\Phi_d}{d_{32}} \quad (28)$$

Where  $\Phi_d$  is the fraction of dispersed phase (aqueous phase) and  $d_{32}$  is the Sauter number (m).

The sauter number can be calculated by the following expression (Zaldívar et al., 1996):

$$\frac{d_{32}}{D_a} = \frac{Af(\Phi_d)}{We^{0.6}} \quad (29)$$

Where  $D_a$  is the diameter of the stirrer (4 cm) and  $A$  is a parameter varying between 0.04 and 4 (Zaldívar et al., 1996).

$We$  is the so-called Webber number, which is equal to:

$$We = \frac{\rho_c n_a^2 D_a^3}{\sigma} \quad (30)$$

Where  $\rho_c$  is the density of the continuous phase ( $\text{kg}\cdot\text{m}^{-3}$ ), which is the organic phase in our system ( $969 \text{ kg}/\text{m}^3$ ),  $n_a$  is the stirring speed ( $\text{s}^{-1}$ ) which is equal to  $6.16 \text{ s}^{-1}$  (370 rpm),  $\sigma$  is the surface tension ( $\text{N}\cdot\text{m}^{-1}$ ) of the system.

The function  $f(\Phi_d)$  (Delichatsios and Probstein, 1976) is equal to:

$$f(\Phi_d) = \left[ \frac{\ln(C_2 + C_3\Phi_d)}{\ln C_2} \right]^{-3} \quad (31)$$

Where  $C_2$  is 0.011 and  $C_3 \rightarrow 1$  on case of  $\Phi_d > 3$ . This function can be represented in two ways, both of which account for re-dispersion and coalescence effects.



### *Calculation of the surface tension*

According to the Good and Girifalco's model (1960), the surface tension can be calculated as:

$$\sigma = \gamma_c + \gamma_d - 2\phi\sqrt{\gamma_c\gamma_d} \quad (32)$$

Where  $\gamma_c$  and  $\gamma_d$  are the surface tension of the continuous and dispersed phase respectively. For the sake of simplicity, the surface tension of the continuous phase was supposed to be the same as the valeric acid, and surface tension for the dispersed to be the same as hydrogen peroxide (Yaws, 1999).

$$\gamma_c[\text{N/m}] = \frac{56.8}{1000} \cdot \left(1 - \frac{T[\text{K}]}{651}\right)^{1.2257} \quad (33)$$

$$\gamma_d[\text{N/m}] = \frac{141.031}{1000} \cdot \left(1 - \frac{T[\text{K}]}{730.15}\right)^{1.2222} \quad (34)$$

The interaction parameter  $\phi$  is calculated according to the mean molar volumes of continuous ( $V_{m,c}$ ) and dispersed phase ( $V_{m,d}$ ):

$$\phi = \frac{4 * [V_{m,c} V_{m,d}]^{1/3}}{\left[V_{m,c}^{1/3} + V_{m,d}^{1/3}\right]^2} \quad (35)$$

At 40°C the interfacial surface area can be estimated to 0.019 N/m for the perhydrolysis of valeric acid.

### *Estimation of diffusion coefficient in mixed solvent*

The Perkins-Geankoplis (1969) equation estimates the diffusion coefficient of a solute in a liquid-liquid system:



$$\begin{aligned}
 D_{m-i}^0 \mu_m^{0.8} &= \sum_{\substack{X=1 \\ X \neq A}} x_X D_{X-i}^0 \mu_X^{0.8} \\
 &= x_{\text{org}} D_{\text{org}-i}^0 \mu_{\text{org}}^{0.8} + x_{\text{aq}} D_{\text{aq}-i}^0 \mu_{\text{aq}}^{0.8}
 \end{aligned} \tag{36}$$

Where  $D_{m-i}^0$  and  $D_{X-i}^0$  are the diffusion coefficients in the mixed solvent and in pure solvent, respectively. The viscosity of the solution can be calculated by:

$$\begin{aligned}
 \ln \mu_m &= \sum_{i=1}^n x_i \ln \mu_i \\
 &= x_{\text{org}} \ln \mu_{\text{org}} + x_{\text{aq}} \ln \mu_{\text{aq}}
 \end{aligned} \tag{37}$$

For the sake of simplicity, the viscosities of the organic and aqueous phase were assumed to be equal to the viscosity of water and valeric acid respectively (Yaws, 1999).

$$\mu_{\text{org}} (\text{cP}) = \mu_{\text{valeric acid}} = 10^{-7.9425 - \frac{1.4583 \cdot 10^3}{T(\text{K})} + 1.5088 \cdot 10^{-2} T(\text{K}) - 1.2781 \cdot 10^{-5} (T(\text{K}))^2} \tag{38}$$

$$\mu_{\text{aq}} (\text{cP}) = \mu_{\text{water}} = 10^{-10.2158 - \frac{1.7925 \cdot 10^3}{T(\text{K})} + 1.7730 \cdot 10^{-2} T(\text{K}) - 1.2631 \cdot 10^{-5} (T(\text{K}))^2} \tag{39}$$

Based on the study of Liu et al. (2004), the correlation of Hayduk-Laudie (1974) can be used to calculate the diffusion coefficients of the component in the aqueous phase (Eq. (40)), and the correlation of Scheibel (1954) (Eq. (41)) to calculate the diffusion coefficients of the component in the organic phase.

$$D_{X-i}^0 [\text{cm}^2 \text{s}^{-1}] = D_{\text{aq}-i}^0 [\text{cm}^2 \text{s}^{-1}] = \frac{13.26 \cdot 10^{-5}}{\mu_{\text{aq}}^{1.4} [\text{cP}] V_i^{0.589} [\text{cm}^3 \text{mol}^{-1}]} \tag{40}$$

$$D_{X-i}^0 [\text{cm}^2 \text{s}^{-1}] = D_{\text{org}-i}^0 [\text{cm}^2 \text{s}^{-1}] = \frac{8.2 \cdot 10^{-8} T [\text{K}]}{\mu_{\text{org}} [\text{cP}] V_i^3 [\text{cm}^3 \text{mol}^{-1}]} \left[ 1 + \left( \frac{3V_{\text{org}} [\text{cm}^3 \text{mol}^{-1}]}{V_i [\text{cm}^3 \text{mol}^{-1}]} \right)^{\frac{2}{3}} \right] \tag{41}$$

Where  $V_i$  is the molar volume at boiling point of the solute.

Figures 16, 17 and 18 show the values of the diffusion coefficients calculated at different temperature for each component of the system.

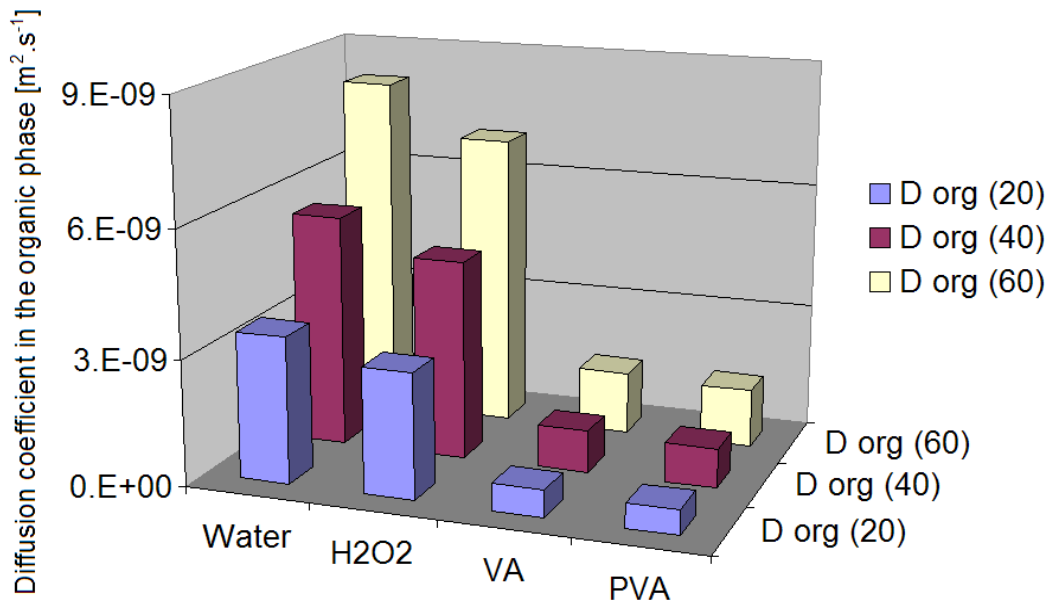


Figure 16 - Diffusion coefficient of different compounds in the organic phase at different temperatures.

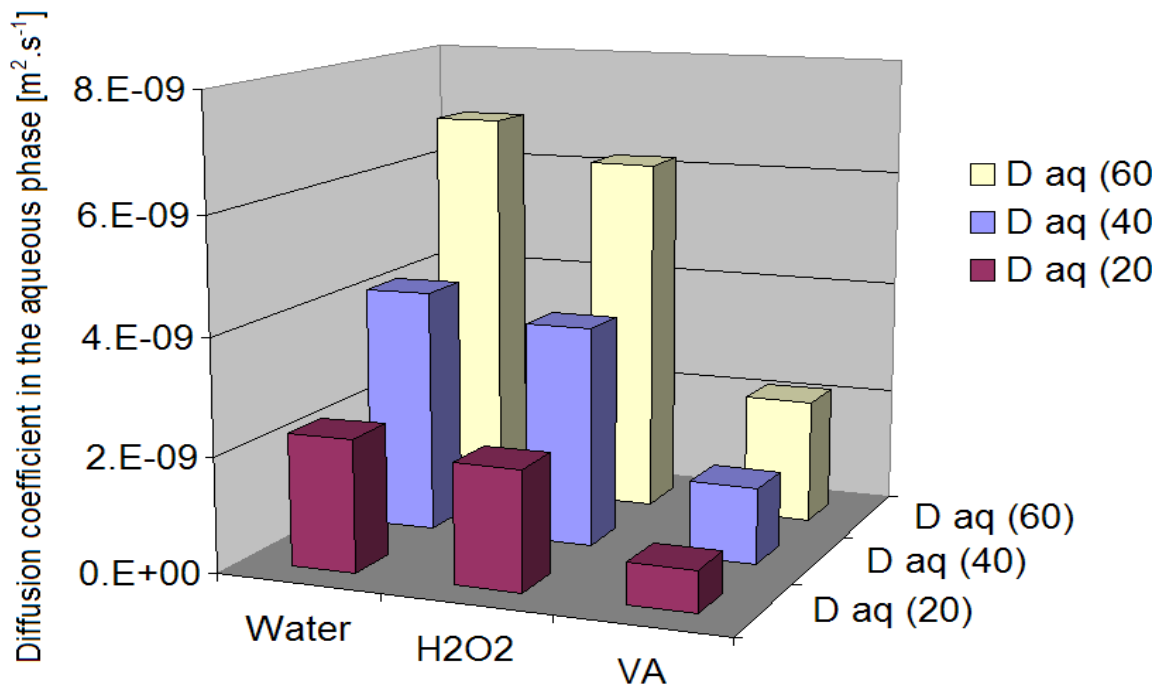
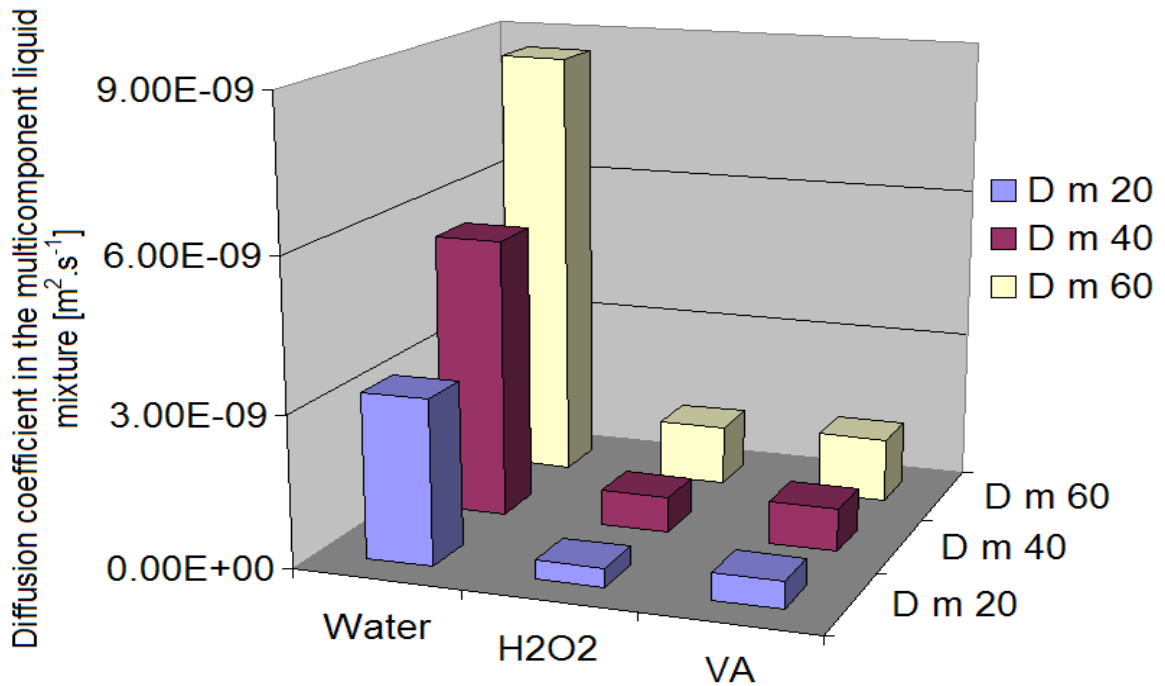


Figure 17 - Diffusion coefficient of different compounds in the aqueous phase at different temperatures.



**Figure 18** - Diffusion coefficient of different compounds in the liquid-liquid system at different temperatures.

#### *Calculation of the mass transfer coefficient in the continuous organic phase*

The mass transfer coefficient for the continuous organic phase was calculated by using the Calderbank and Moo-Young (1961) relation:

$$k_{c-i} = 1.310^{-3} \left[ \frac{P\mu_c}{V_c\rho_c^2} \right]^{\frac{1}{4}} \left[ \frac{\mu_c}{\rho_c D_{m-i}} \right]^{\frac{-2}{3}} \quad (42)$$

The viscosity of the continuous organic phase  $\mu_c$  ( $\text{kg}\cdot\text{m}^{-3}\cdot\text{s}$ ) was estimated by (38). The density  $\rho_c$  ( $\text{kg}\cdot\text{m}^{-3}$ ) and volume  $V_c$  ( $\text{m}^3$ ) were calculated experimentally.

$P$  ( $\text{kg}\cdot(\text{s}^3\text{m}^2)^{-1}$ ) represents the power dissipated by the stirrer and it is equal to:

$$P = \psi\rho_m n_a^3 D_a^5 \quad (43)$$

Where  $\psi$  is the power consumption number of the stirrer equal to 1.5 (Houncine et al., 2000) and  $\rho_m$  ( $\text{kg}\cdot\text{m}^{-3}$ ) is the density of the mixture equal to  $\phi_c V_c + \phi_d V_d$ .



$D_{m-I}$  is the diffusion coefficient in the multicomponent liquid mixture calculated in the previous section.

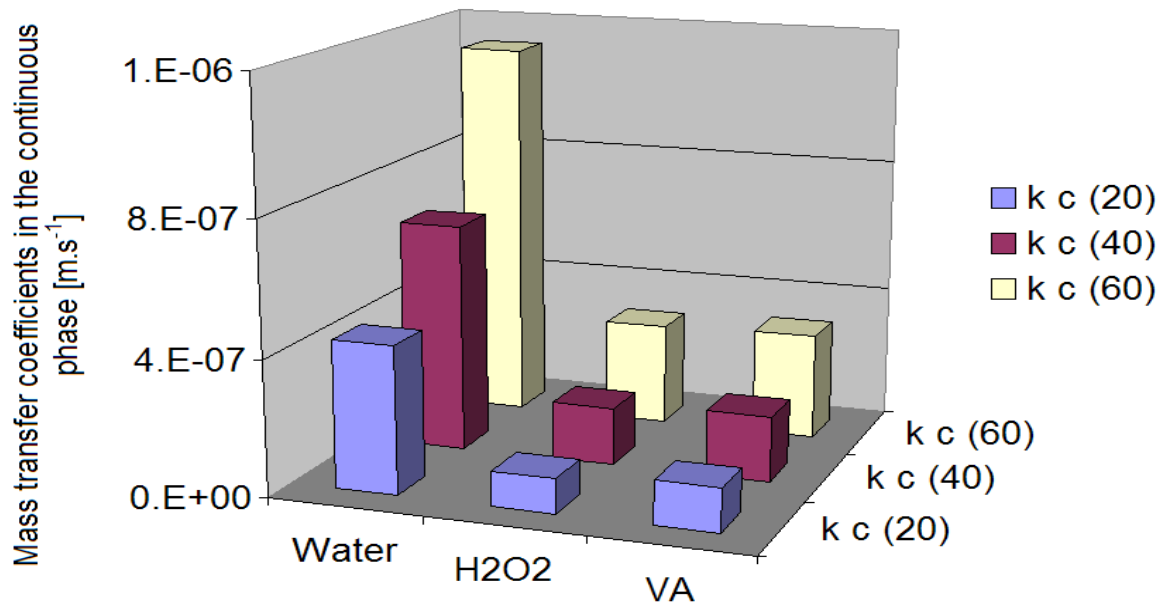


**Figure 19** - Mass transfer coefficients in the organic phase.

#### *Calculation of the mass transfer coefficient in the dispersed aqueous phase*

The mass transfer coefficient of the dispersed phase depends on the drop behavior: mostly upon whether the drop is rigid or not. To be able to evaluate the latter, the diameter number ( $d^*$ ) must be calculated (van Woezik and Westerterp, 2000).

$$d^* = d_{32} \left[ \frac{\mu_c^2}{\rho_c g \Delta\rho} \right]^{-1/3} \quad (44)$$

Where  $g$  is the gravity acceleration ( $m.s^{-2}$ ) and  $\Delta\rho = \rho_c - \rho_d$ .

For the drop to be considered as rigid sphere,  $d^*$  must be less than 10. Indeed, for a rigid sphere Treybal gives the following correlation:



$$k_{d-i} = \frac{2\pi^2 D_{m-i}}{3 d_{32}} \quad (45)$$

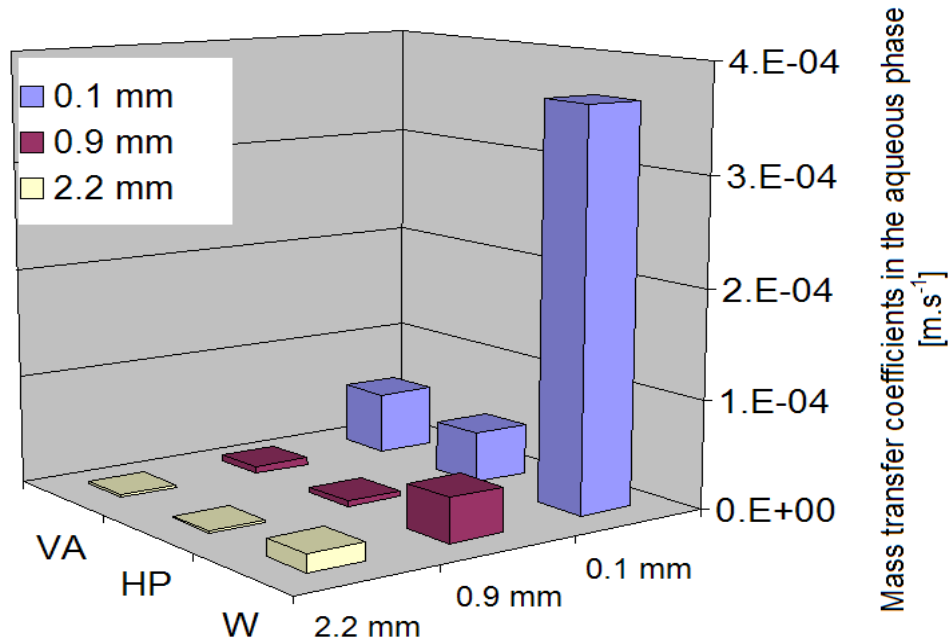


**Figure 20** – Mass transfer coefficients in the aqueous phase at 40°C vs  $d_{32}$ .

### *Modeling and results*

The software MODEST [13] was used for the estimation of  $k_{het}$  and  $E_a$  parameters. The Simplex and Levenberg-Maquardt algorithms were used to minimize the objective function  $\theta$ :

$$\theta = \sum \left( y_i - \hat{y}_i \right)^2 \quad (46)$$

Where  $y_i$  is the experimental value of concentration and  $\hat{y}_i$  is the concentration predicted by the model.

The general equation for a batch reactor is set for all the compounds in our system:





$$\begin{aligned}
 r_{VA} &= \frac{d[VA]}{dt} = -r_{tot} \\
 r_{PVA} &= \frac{d[PVA]}{dt} = r_{tot} \\
 r_{H_2O_2} &= \frac{d[H_2O_2]}{dt} = -r_{tot} \\
 r_{H_2O} &= \frac{d[H_2O]}{dt} = r_{tot}
 \end{aligned}
 \tag{47}$$

These equations combined with the mass balance were solved numerically during the parameter estimation.

A modified Arrhenius equation is used for describing the temperature dependence of the homogeneous rate of reaction  $k_{hom}$ :

$$k_{hom} = k_{ave} \exp\left(\frac{-Ea}{R} \left(\frac{1}{T} - \frac{1}{T_{ave}}\right)\right)
 \tag{48}$$

Where  $T_{ave}$  is the average temperature of the experiments, 45°C, and  $k_{ave}$  is calculated as follows:

$$k_{ave} = A \exp\left(\frac{-Ea}{RT}\right)
 \tag{49}$$

This modification in the Arrhenius equation was done in order to minimize the correlation between the frequency factor and the activation energy during the parameter estimation.

A summary of the general results obtained is shown in tables 5 and 6.

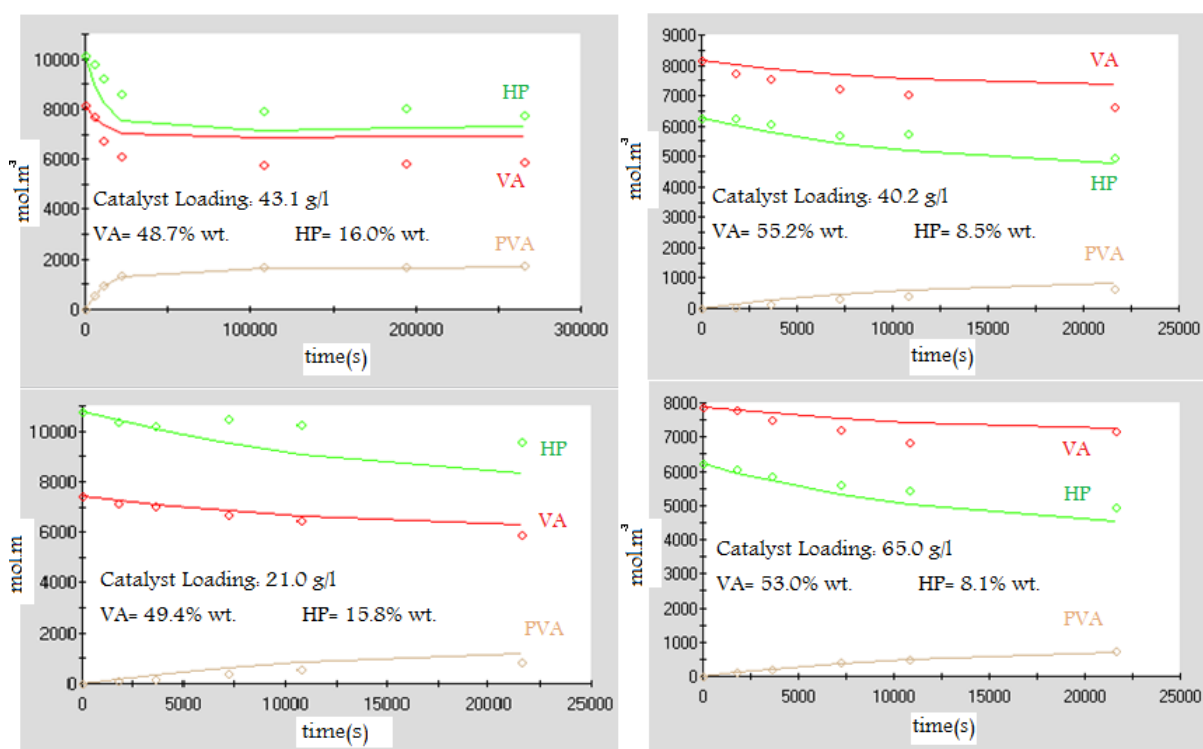
**Table 4** - Kinetic parameters estimated

Parameters	Estimation	Errors(%)
$k_{het}(\text{L}\cdot\text{mol}^{-1}\cdot\text{g}^{-1}\cdot\text{s}^{-1})$	$0.74 \cdot 10^{-10}$	13.7
Ea (kJ/mol)	63.6	23.2

**Table 5** - Thermodynamic parameters calculated

Parameters	Estimation
$K_{eq}$ (at 40°C)	2.1
$\Delta H_r^o$ (kJ/mol)	-13.8

The modeling results are presented in figure 21 and 22.

**Figure 21** - Fit of the model for the perhydrolysis of valeric acid at 60°C and 370 rpm.

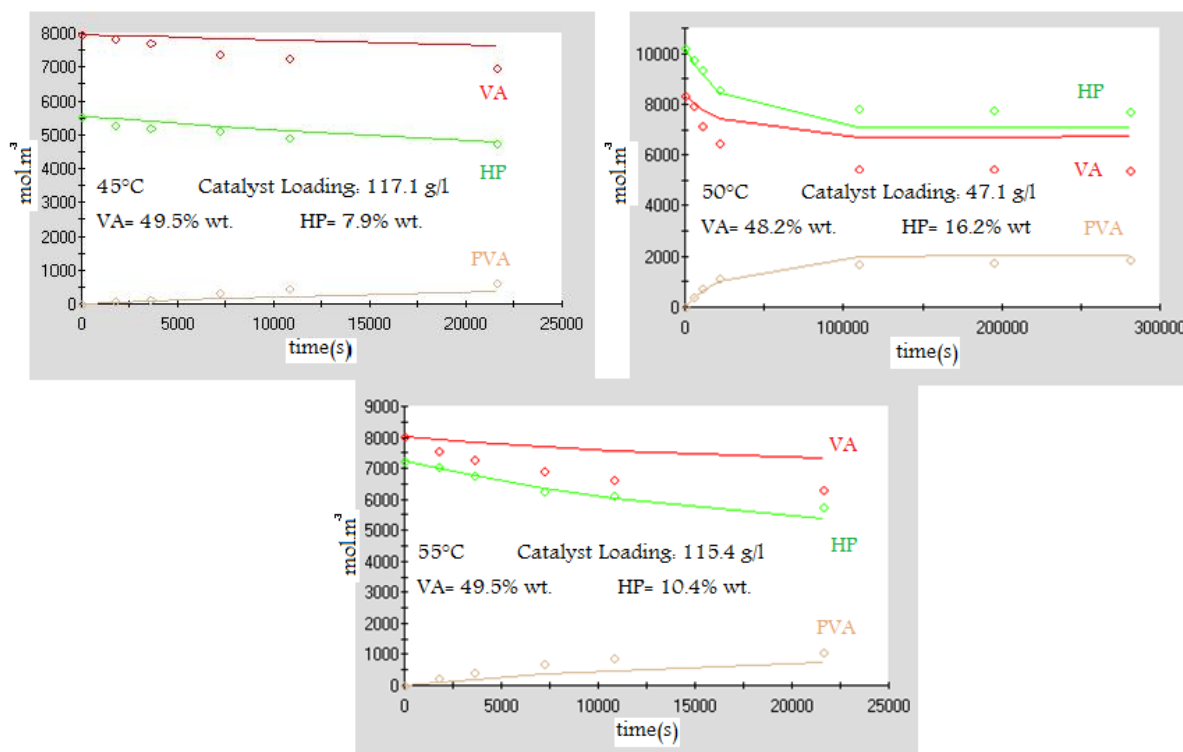


**Figure 22** - Fit of the model for the perhydrolysis of valeric acid at different temperatures and 370 rpm.

Due to the biphasic nature of our reaction system, one cannot compare directly the values estimated by our model with the perhydrolysis in monophasic media, which have few data published in the literature. However, it was found that the energy of activation required for the peroxyvaleric acid synthesis (63.4 kJ/mol) is higher than for the synthesis of peroxyacetic acid (42.5 kJ/mol) and peroxy propionic acid (51.4 kJ/mol). Since the perhydrolysis of fatty acids is considerably slower this result corresponds with our expectation.

The simplified model for the heterogeneous reaction proposed in equation (11) showed to be quite satisfactory for describing the generation of PVA in our system. However, the consumption of VA and HP presented a considerable deviation in some experiments. The reason for that is not certain yet, but one knows that some improvements shall be done in the model to get more precise results. Such improvements could be done by adding further information about the enthalpy of reaction, a deeper analysis of the non-ideality of the system and its influence in the  $K^c$  and a more detailed model for the heterogeneous reaction covering



the intra-particle concentration approach. It would be interesting if these parameters could be easily calculated by some computational thermodynamic model; however, unfortunately there is a lack of data concerning the influence of the peroxide group.



## 5 Conclusions

The present work has demonstrated that the perhydrolysis of valeric acid is feasible and occurs even in the absence of catalyst, although the heterogeneous catalyst, Amberlite IR-120, performed a significant increase in the kinetics and conversion of the reaction.

The influence of the stirring speed was analyzed for kinetic experiments at 207, 370, 500 and 800 rpm. Below 207 rpm the catalyst particles were not able to be suspended all over the reactor and over 800 rpm the system got too much instable, presenting vibrations and some catalyst particles were launched to the roof of the reactor. Therefore, the velocities of 207 and 370 rpm showed that the reaction was already in the kinetic regime. The experiments carried out at 500 and 800 rpm showed a smaller conversion compared to the others: one can assume this is due to a vortex created that pushes the catalyst against the reactor walls.

The internal mass transfer effect was tested by using two catalysts with different particle sizes than Amberlite IR-120 but with the same degree of cross linking, matrix and active sites. Dowex 50x8-400 and Dowex 50x8-50 have demonstrated that the internal mass transfer effect is negligible.

An experimental method was developed with the aim to find the concentration of components inside the catalyst particles. The method is based in several catalyst washes followed by the analysis of the filtrated liquid. The results are quite promising; however there was not enough time to include this parameter in the present kinetic model.

The kinetic model developed took into account the mass transfer between the organic and the aqueous phase. The results obtained presented a good agreement for most of the experiments modeled, especially for the production of peroxyvaleric acid. Further investigations about the non-ideality of the system, the enthalpy of reaction and the heterogeneous mechanism of reaction should be done in order to improve the accuracy of the kinetic model.



## 6 Acknowledgements

The financial support from Åbo Akademi and CAPES is gratefully acknowledge.



## 7 Notation

$A$	interfacial area [ $\text{m}^2$ ]
$a_o$	mass transfer-to-volume ratio [ $\text{m}^2 \cdot \text{m}^{-3}$ ]
$CL$	catalyst loading [ $\text{g} \cdot \text{m}^{-3}$ ]
$d_{32}$	Sauter number [m]
$D_a$	diameter of the stirrer [m]
$D_{m-i}^0$	diffusion coefficients of $i$ in the mixed solvent [ $\text{cm}^2 \cdot \text{s}^{-1}$ ]
$D_{X-i}^0$	diffusion coefficients of $i$ in the pure solvent [ $\text{cm}^2 \cdot \text{s}^{-1}$ ]
$d^*$	diameter number [m]
$E_a$	activation energy [ $\text{J} \cdot \text{mol}^{-1}$ ]
$G$	Gibbs energy [ $\text{kJ} \cdot \text{mol}^{-1}$ ]
$g$	gravity acceleration [ $\text{m} \cdot \text{s}^{-2}$ ]
$\Delta H_R^\circ$	standard enthalpy change of reaction [ $\text{kJ} \cdot \text{mol}^{-1}$ ]
$[i]$ or $c_i$	concentration of $i$ [ $\text{mol} \cdot \text{L}^{-1}$ ]
$k$	rate constant [ $\text{L} \cdot \text{mol}^{-1} \cdot \text{s}^{-1}$ ]
$k_{\text{het}}$	rate constant [ $\text{L} \cdot \text{mol}^{-1} \cdot \text{g}^{-1} \cdot \text{s}^{-1}$ ]
$k_D$	mass transfer coefficient [ $\text{m} \cdot \text{s}^{-1}$ ]
$k_{\text{org-}i}$	mass transfer coefficient for $i$ in the organic phase [ $\text{m} \cdot \text{s}^{-1}$ ]
$k_{\text{org-i}}$	mass transfer coefficient for $i$ in the aqueous phase [ $\text{m} \cdot \text{s}^{-1}$ ]



$K_i$	distribution coefficient
$K^C$	equilibrium constant, based on concentrations
$K^T$	true thermodynamic constant, based on activities
$n_a$	stirring speed [ $s^{-1}$ ]
$N$	flux [ $mol \cdot m^{-2} \cdot s^{-1}$ ]
$n$	amount of substance [mol]
$P$	power dissipated by the stirrer [ $kg \cdot (s^3 m^2)^{-1}$ ]
$Q$	reaction quotient
$R$	gas constant [ $J \cdot mol^{-1} \cdot K^{-1}$ ]
$r_{tot}$	total rate of reaction
$r_{hom}$	homogeneous rate of reaction
$r_{het}$	heterogeneous rate of reaction
$T$	temperature
$x$	mole fraction
$V_i$	molar volume at boiling point of the solute [ $m^3 \cdot mol^{-1}$ ]
$V$	volume [ $m^3$ ]
$V_{o,tot}$	total volume measured in the end of the reaction [ $m^3$ ]
Greek letters	
$\theta$	objective function
$\mu_f$	viscosity of the fluid [ $Ns \cdot m^{-2}$ ]





$\rho_f$	fluid density [ $\text{kg}\cdot\text{m}^{-3}$ ]
$\Phi_d$	fraction of dispersed phase
$\psi$	power consumption number of the stirrer
$\sigma$	surface tension [ $\text{N}\cdot\text{m}^{-1}$ ]

Dimensionless groups

We	Webber number $We = \frac{\rho_c n_a^2 D_a^3}{\sigma}$
----	--



## 8 References

Pruss, A.; Hansen, A.; Kao, M.; Gürtler, L.; Pauli, G.; Benedix, F.; von Versen, R.; Cell and Tissue Banking, 2, 201-215 (2001).

Ölmez, H.; Kretzschmar, U.; Food Sci. Technology, 42, 686-693 (2009).

Kitis M.; Environ. Int., 30, 47-55 (2004).

Polonca, P.; Tavčer, P. T. ; Color. Technol., 124, 36-42 (2008).

Goud, V. V.; Patwardhan, A. V.; Dinda, S.; Pradhan, N. C.; Chem. Eng. Sci., 62, 4065-4076 (2007)

Nardello-Rataj, V.; Tai, L. H. T.; Aubry, J. M.; L'Actualité Chimique (2003),

Campanella, A.; Baltanas, M. A.; “*Degradation of oxirane ring of epoxidized vegetable oils in liquid-liquid heterogeneous reaction systems*”, Chem. Eng. Journal, 118, 141-152 (2006).

Leveneur, S.; Murzin, D. Yu.; Salmi, T.; Mikkola, J.-P.; Kumar, N.; Eränen, K.; Estel, L.; ”*Synthesis of peroxypropionic acid from propionic acid and hydrogen peroxide over heterogeneous catalysts*”, Chem. Eng. J., 147, 323-329, (2009).

Leveneur, S; Wärnå, J.; Salmi, T.; Murzin, D. Yu.; Estel, L.; “*Interaction of intrinsic kinetics and internal mass transfer in porous ion-exchange catalysts: green synthesis of peroxy-carboxylic acids*”. Chem. Eng. Sci., 64, 4104-4114, (2009).

Musante, R.L.; Grau, R.J.; Baltanas, M.A.; “*Kinetic of liquid-phase reactions catalyzed by acidic resins: the formation of peracetic acid for vegetable oil epoxidation*”, Appl. Catal., 197, 165-173, (2000).



Sue, K.; Ouchi, F.; Minami, K.; Arai, K.; “*Determination of carboxylic acid dissociation constants to 350°C at 23MPa by potentiometric pH measurements*“, J. Chem. Eng. Data., 49, 1359-1363, (2004).

Altiokka, M.R.; “*Kinetics of hydrolysis of benzaldehyde dimethyl acetal over Amberlite IR-120*“, Ind. Eng. Res., 46, 1058-1062, (2007).

Cantieni, R.; “*Photochemical peroxide formation. VII. Oxidation of acetic, propionic, butyric and isovaleric acids by means of molecular oxygen in ultraviolet light*“, Zeitschrift fuer Wissenschaftliche Photographie, Photophysik und Photochemie, 36, 90-95 (1937).

Greenspan, F.P.; Mackellar, D.G.; “*Analysis of aliphatic per acids*“, Anal. Chem., 20, 1061-1063, (1948).

Hawkinson, A.T.; Schitz, W.R.; “*Improvements in or relating to the oxidation of aliphatic carboxylic acids to peracids*“, Adv. Science Tech., 39, 350-382, (2004).

Levenspiel, O.; Chemical Reaction Engineering. 3rd ed. New York: John Wiley & Sons Inc., (1999).

Phillips, B.; Starcher, P. S.; Ash, B.D.; “*Preparation of aliphatic peroxyacids*“, J. Org. Chem., 23, 1823-1826 (1958).

Rüsch gen. Klaas, M.; Steffens, K.; Patett, N.; “*Biocatalytic peroxy acid formation for disinfection*“, J. Mol. Catal. B-Enzym., 19-20, 499-505 (2002).

Saha, M.S; Nishiki, Y.; Furuta, T.; Denggerile, A.; Ohsaka, T.; “*A new method for the preparation of peroxyacetic acid using solid superacid catalysts*“, Tetrahedron Lett. , 44, 5535-5537, 2003.

Salmi T.O.; Mikkola J.-P.; Wärnå J.P.; Chemical reaction engineering and reactor technology, 1st Ed. Turku: CRC Press (2010).

Trambouze, P.; Euzen, J.-P.; Les Réacteurs Chimiques. 2<sup>nd</sup> Ed., Paris : Editions TECHNIP (2002).



Villermaux, J. ; Génie de la Réaction Chimique. 2nd ed., Paris : Tec&Doc Lavoisier (1993).

Pan, G. X. ; Spencer, L. ; Leary, G. J. ; *Holzforschung*, 54, 144-152 (2000).

Pan, G. X. ; Spencer, L. ; Leary, G. J. ; *Holzforschung*, 54, 153-158 (2000).

Zaldívar, J. M. ; Molga, E. ; Alós, M. A. ; Hernández, H. ; Westerterp, K. R. ; “*Aromatic nitrations by mixed acid, slow liquid-liquid reaction regime*”, *Chem. Eng. Process*, 35, 91-105 (2006) .

Sawistowski, H. ; “*Physical aspects of liquid-liquid extraction, in: Proceedings with NATO in Mass Transfer with Chemical Reaction in Multiphase Systems*”, Istanbul, Turkey (2001).

Van Woezik, B. A. A. ; Westerterp, K. R. ; “*Measurement of interfacial areas with chemical method for a system with alternating dispersed phases*”, *Chem. Eng. Process*, 39, 299-314 (2000).

Delichatsios, M. A.; Probst, R. F.; “*The effect of coalescence on the average drop size in liquid-liquid dispersions*”, *Ind. Eng. Chem. Fundam.*, 15, 134-138 (1976).

Calderbank, P. H.; Moo-Young, M. B.; “*The continuous phase heat and mass-transfer properties of dispersions*”, *Chem. Eng. Sci.*, 16, 39-54 (1961).

Treybal, R. E.; *Liquid Extraction*, second ed., McGraw-Hill, New York, NY (1963).